

**PREPARATION OF HYDROTHERMAL  
SYNTHESIZED LEAD TITANATE FILM FOR  
NON-VOLATILE MEMORY DEVICE  
APPLICATION**

**PhD DISSERTATION**

**THIN THIN THWE**

**DEPARTMENT OF PHYSICS  
UNIVERSITY OF YANGON  
MYANMAR**

**APRIL 2012**

## **ACKNOWLEDGEMENTS**

I would like to thank Professor Dr Win Win Thar PhD (UY) Head of Department of Physics, University of Yangon, for her kind permission to carry out this study.

I gratefully thank Supervisor Dr Yin Maung Maung PhD (UY) Lecturer, Department of Physics, University of Yangon.

I would like to thank Co. supervisor Dr Than Than Win PhD (UY) Lecturer, Department of Physics, University of Yangon.

**PREPARATION OF HYDROTHERMAL  
SYNTHESIZED LEAD TITANATE FILM FOR  
NON-VOLATILE MEMORY DEVICE  
APPLICATION**

**PhD DISSERTATION**

**THIN THIN THWE**

**DEPARTMENT OF PHYSICS  
UNIVERSITY OF YANGON  
MYANMAR**

**APRIL 2012**

## **ABSTRACT**

Lead titanate ultra-fine powder is prepared by hydrothermal synthesis at different temperatures (160°C - 190°C). Scanning Electron Microscopy is used to study the microstructure of lead titanate powder. Capacitance and voltage (C-V) characteristics of lead titanate ceramic capacitor is measured by impedance analyzer. Lead titanate film is formed on Si – substrate by single wafer spin processor. Morphology and film thickness are examined by SEM. The I(V), C(V),  $C^{-2}(V)$  and P(E) characteristics are investigated for electrical and ferroelectric properties.

3.7	C <sup>2</sup> -V Characteristics of Lead Titanate Film	23
3.8	P-E Hysteresis Loop Measurement	24
<b>CHAPTER IV CONCLUSION</b>		<b>64</b>
<b>REFERENCES</b>		<b>66</b>

## LIST OF FIGURE

<b>Figure</b>	<b>Page</b>
2.1 (a) Lead (II) Nitrate	6
2.1 (b) Titanium Dioxide	7
2.1 (c) Potassium Hydroxide	8
2.1 (d) Teflon – lined Stainless Steel Bomb	9
2.2 (a) Mixing the Starting Reagents	10
2.2 (b) Stir with Glass Rod	11
2.2 (c) Pour Mix Solution into Stainless Steel Bomb	12
2.2 (d) Hydrothermal Bath	13
2.3 (a) Same Colour of PbTiO <sub>3</sub> Powders	14
2.3 (b) The Magnetic Stirrer	15
2.3 (c) The Photograph of Spin Coating System of the Spin Processor (MODEL WS-400BZ- 6N PP/LITE)	16
2.3 (d) Single Wafer Spin Processor 17	
2.3 (e) The PbTiO <sub>3</sub> /p-Si Structure Process Temperature	18
2.4 Experimental Procedure	19
3.1 (a) XRD Profile for PbTiO <sub>3</sub> Powder at 160°C	27
3.1 (b) XRD Profile for PbTiO <sub>3</sub> Powder at 170°C	28
3.1 (c) XRD Profile for PbTiO <sub>3</sub> Powder at 180°C	29
3.1 (d) XRD Profile for PbTiO <sub>3</sub> Powder at 190°C	30
3.2 (a) SEM Image for PbTiO <sub>3</sub> Powder at 160°C	31
3.2 (b) SEM Image for PbTiO <sub>3</sub> Powder at 170°C	32
3.2 (c) SEM Image for PbTiO <sub>3</sub> Powder at 180°C	33
3.2 (d) SEM Image for PbTiO <sub>3</sub> Powder at 190°C	34
3.3 (a) C-V Characteristics of PbTiO <sub>3</sub> Ceramic at 160°C	35
3.3 (b) C-V Characteristics of PbTiO <sub>3</sub> Ceramic at 170°C	36
3.3 (c) C-V Characteristics of PbTiO <sub>3</sub> Ceramic at 180°C	37
3.3 (d) C-V Characteristics of PbTiO <sub>3</sub> Ceramic at 190°C	38
3.4 (a) SEM Image for PbTiO <sub>3</sub> Film at 500°C	39
3.4 (b) SEM Image for PbTiO <sub>3</sub> Film at 550°C	40

# CONTENT

Page

## ACKNOWLEDGEMENTS

## ABSTRACT

## LIST OF CONTENTS

## LIST OF FIGURE

## LIST OF TABLE

### CHAPTER I INTRODUCTION

1.1	Ferroelectric Materials	1
1.2	Ferroelectric Capacitor Memory Devices	1
1.3	Nonvolatile Ferroelectric Random Access Memory	2
1.4	Hydrothermal Synthesis	2

### CHAPTER II EXPERIMENTAL PROCEDURE

2.1	Preparation of $\text{PbTiO}_3$ Powder	4
2.2	Substrate Preparation	4
2.3	Preparation of $\text{PbTiO}_3$ Film	5

### CHAPTER III RESULTS AND DISCUSSION

3.1	Phase Formation of $\text{PbTiO}_3$ powder	20
3.1.1	Lattice parameters, Lattice distortion and Cell Volume	20
3.1.2	Crystallite size (Nano-particle size)	21
3.2	Microstructural study by SEM	21
3.3	C-V Characteristics of Lead Titanate ceramic capacitor	22
3.4	Morphology and film thickness by SEM	22
3.5	I-V Characteristics of $\text{PbTiO}_3$ films	22
3.6	C-V Characteristics of $\text{PbTiO}_3$ films (Nonvolatile memory nature)	23

## LIST OF TABLE

<b>Table</b>	<b>Page</b>
3.1 Lattice Parameters for both Standard and Observed Values	20
3.2 Lattice Strain / Tetragonality of both Values	21
3.3 Crystallite Size at Different Annealing Temperatures	21
3.4 Some Diode Parameters of PbTiO <sub>3</sub> Films at Different Process Temperatures	23
3.5 Width of Memory Window at Different Process Temperatures	23
3.6 The Relationship of Reaction Temperature and N <sub>a</sub> , W and V <sub>bi</sub>	24
3.7 P <sub>r</sub> , P <sub>s</sub> and E <sub>c</sub> Different Temperature	26

3.4 (c)	SEM Image for PbTiO <sub>3</sub> Film at 600°C	41
3.4 (d)	SEM Image for PbTiO <sub>3</sub> Film at 650°C	42
3.4 (e)	Film Thickness of SEM Image for PbTiO <sub>3</sub> Film at 500°C	43
3.4 (f)	Film Thickness of SEM Image for PbTiO <sub>3</sub> Film at 550°C	44
3.4 (g)	Film Thickness of SEM Image for PbTiO <sub>3</sub> Film at 600°C	45
3.4 (h)	Film Thickness of SEM Image for PbTiO <sub>3</sub> Film at 650°C	46
3.5 (a)	I-V Characteristics of PbTiO <sub>3</sub> Films at Different Process Temperatures	47
3.5 (b)	lnI-V Characteristics of PbTiO <sub>3</sub> Films	48
3.6 (a)	C-V Characteristics of PbTiO <sub>3</sub> Film at 500°C	49
3.6 (b)	C-V Characteristics of PbTiO <sub>3</sub> Film at 550°C	50
3.6 (c)	C-V Characteristics of PbTiO <sub>3</sub> Film at 600°C	51
3.6 (d)	C-V Characteristics of PbTiO <sub>3</sub> Film at 650°C	52
3.7 (a)	C <sup>-2</sup> -V Characteristics of PbTiO <sub>3</sub> (160°C)/ p-Si Process Temperature at 500°C	53
3.7 (b)	C <sup>-2</sup> -V Characteristics of PbTiO <sub>3</sub> (170°C)/ p-Si Process Temperature at 550°C	54
3.7 (c)	C <sup>-2</sup> -V Characteristics of PbTiO <sub>3</sub> (180°C)/ p-Si Process Temperature at 600°C	55
3.7 (d)	C <sup>-2</sup> -V Characteristics of PbTiO <sub>3</sub> (190°C)/ p-Si Process Temperature at 650°C	56
3.8 (a)	P-E Hysteresis Loop of PbTiO <sub>3</sub> Film at 500°C	57
3.8 (b)	P-E Hysteresis Loop of PbTiO <sub>3</sub> Film at 550°C	58
3.8 (c)	P-E Hysteresis Loop of PbTiO <sub>3</sub> Film at 600°C	59
3.8 (d)	P-E Hysteresis Loop of PbTiO <sub>3</sub> Film at 650°C	60
3.9 (a)	Polarization reversal at Different Process Temperatures	61
3.9 (b)	Spontaneous Polarization Density at Different Temperatures	62
3.9 (c)	The Change in E <sub>c</sub> with Respect to Process Temperature	63

### **1.3 Nonvolatile Ferroelectric Random Access Memory**

Ferroelectric random access memory (FeRAM) has shown much potential in replacing volatile dynamic random access memory (DRAM), the current choice for computer technology. FeRAM is nonvolatile, meaning that the charge stored upon the bit capacitor is stable, negating the need for an energy-intensive data refresh. Thus, for portable applications where energy is limited, FeRAM is attracting significant interest. Dynamic random access memory (DRAM) is commonly used in most of today's computer technology. However, it is volatile, meaning that it must have access to a power source at all times, and any data stored upon it must constantly be refreshed in order to maintain it. As ferroelectric random access memory (FeRAM) is nonvolatile, it does not need constant access to a power source, giving it an advantage over DRAM in terms of power conservation. Fatigue, which is one of the reliability issues encountered with FeRAM will be studied in the ferroelectric lead titanate  $\text{PbTiO}_3$  thin films in this work. Fatigue is defined as the loss of switchable polarization with repeated switching. The switchable polarization is derived from the electric field-driven movement within each unit cell of the body-centered cation either up or down relative to the oxygen anions. The polarization charge translates to a one or zero stored on a computer memory's capacitor, which is made of a ferroelectric material sandwiched between two metal electrodes. [6]

### **1.4 Hydrothermal Synthesis**

Hydrothermal synthesis includes the various techniques of crystallizing substances from high-temperature aqueous solution at high vapor pressures, also termed "hydrothermal method". It can be defined as a method of synthesis of single crystals, which depends on the solubility of minerals in hot water under high pressure. The temperature can be elevated above the boiling point of the water, reaching the pressure of vapor saturation [7]. One of the main advantages of hydrothermal synthesis is the ability to control the grain size by varying the synthesis temperature and concentrating of hydrothermal bath [8].

# CHAPTER I

## INTRODUCTION

### 1.1 Ferroelectric Materials

Ferroelectric materials are very often dielectric. For most applications of ferroelectric materials the dielectric constant and dielectric loss are important practical parameters [1]. Ferroelectric materials, in particular ceramics, have been commercially important to the electronics industry for more than 50 years [2]. Ferroelectric materials can be used in different ways in memory designs. The first use is a thin film of ferroelectric in a capacitor as a non-volatile storage element using the hysteresis property of polarization versus voltage as the means of storing data [3].

All ferroelectric materials have a transition temperature called the Curie ( $T_c$ ). At a temperature  $T > T_c$  the crystal does not exhibit ferroelectricity, while for  $T < T_c$  it is ferroelectric. On decreasing the temperature through the Curie point, a ferroelectric crystal undergoes a phase transition from a non-ferroelectric phase a ferroelectric phase. If there are more than one ferroelectric phases, the temperature at which the crystal transforms from one ferroelectric phase to another is called the transition temperature [4].

### 1.2 Ferroelectric Capacitor Memory Devices

The inherent memory derived from the spontaneous polarization of ferroelectric materials has already been used in ferroelectric memories based on the Dynamic Random Access Memory (DRAM) one transistor/one capacitor (1T/1C) design. All of the exciting developments in FRAM memory technology are finding their way into a host of applications that people use every day Ferroelectric thin films have attracted much attention for potential applications such as high dielectric constant capacitors, infrared detectors, piezoelectric transducers, optical modulators, optical waveguides, nonvolatile memory chips and capacitors for dynamic random access memory (DRAM)[5].

## CHAPTER II

### EXPERIMENTAL PROCEDURE

#### 2.1 Preparation of PbTiO<sub>3</sub> Powder

By using the hydrothermal versatile technique, Lead Titanate (PbTiO<sub>3</sub>) powders were produced. These powders were grown by reacting 4 g of lead (II) nitrate (Pb(NO<sub>3</sub>)<sub>2</sub>), 1 g of titanium dioxide (TiO<sub>2</sub>), 1.5 mol of potassium hydroxide (KOH) and 20 ml of deionized water (DIW) in Teflon-lined steel-bomb at different treatment time at 160°C, 170°C, 180°C and 190°C. The starting reagents and experimental accessories were shown in Fig 2.1 (a-d). Firstly KOH, (Pb(NO<sub>3</sub>)<sub>2</sub>), (TiO<sub>2</sub>) and (DIW) were mixed in beaker as shown in Fig 2.2 (a). And then, stir with glass rod as shown in Fig 2.2 (b). After mixing, it was poured into the Teflon-lined stainless steel-bomb as shown in Fig 2.2 (c). The mixture was oven-dried at 160°C for 04:30h, 170°C for 3:30h, 180°C for 3:00h and 190°C for 02:30h in the hydrothermal bath as shown in Fig 2.2 (d). It was found that all the resulting samples have the same colour (dull yellow) in accordance with the same bath morality as shown in Fig 2.3 (a). It might be assumed that, all the samples have the same colour due to the constant bath morality although the treatment temperature were changed.

#### 2.2 Substrate Preparation

The substrates Si (100) were cleaned with HF:H<sub>2</sub>O (1:5) for 15 minutes and dried at room temperature to remove native oxide. Then the substrates were immersed in acetone for 10 minutes and dried in four times. After that, it was immersed in methanol for 5 minutes and dried to remove impurities. Finally, they were cleaned with distilled water for 5 minutes and dried, at room temperature.

Ferroelectricity is a phenomenon that is created when materials with qualities that make them ideal for ferroelectric current to develop have been placed in close proximity exhibit. The resulting creation of electrical flow is referred to as the creation of a dipole moment. Materials that possess ferroelectric properties are physically attached to a lattice grid that can be used as a conductor. Other common devices used in such thing as heat sensors and motion detectors that are commonly used in fire safety and security systems. Even the automobile industry benefits from employing the physics of ferroelectricity [9]. Lead (II) nitrate ( $\text{Pb}(\text{NO}_3)_2$ ) is an inorganic compound, it commonly occurs as a colourless crystal or white powder and unlike most other Lead (II) salts, is soluble in water [10]. Titanium dioxide ( $\text{TiO}_2$ ), also know as titanium (IV) oxide or titania, is the naturally occurring oxide of titanium. It is widely used to provide whiteness and opacity and also used as a semiconductor [11]. Potassium hydroxide (KOH) is highly basic, forming strongly alkali solutions in water and other polar solvents and see also sodium hydroxide. Its dissolution in water is strongly exothermic, leading to a temperature rise, sometimes up to boiling point. KOH is a desiccant. In the laboratory it is particularly useful for drying basic solvents [12]. Lead Titanate ( $\text{PbTiO}_3$ ) is a very attractive material for the use in a wide variety of field, including ultrasonic sensors, infrared detectors, electro-optic modulators, and ferroelectric random access memories [13]. Teflon is known for their excellent chemical resistance, superior electrical properties, and high service temperatures. Stainless steel is a very versatile material. It can literally be used for years and remain stainless [14-15]. In this process, hydrothermal synthesis was demonstrated for the formation of perovskite phase  $\text{PbTiO}_3$  powders. For this reaction Teflon-lined stainless steel bomb was used as a container.

### 2.3 Preparation of PbTiO<sub>3</sub> Film

The PbTiO<sub>3</sub> powder and ethanol were mixed and stirred by magnetic stirrer to get precursor solution as showed in Fig 2.3 (b). And then Precursor solution was deposited on the substrate by spin coating technique as shown in 2.3 (c-d). Later, layer was dried at room temperature. Then, the substrates were annealed at 500°C to 650°C for 1 hr by conventional annealing process. Finally Cu/PbTiO<sub>3</sub>/Si structure was formed and given as Fig 2.3 (e). The procedure for preparation of PbTiO<sub>3</sub> films by spin-coating technique was shown in Fig 2.4.

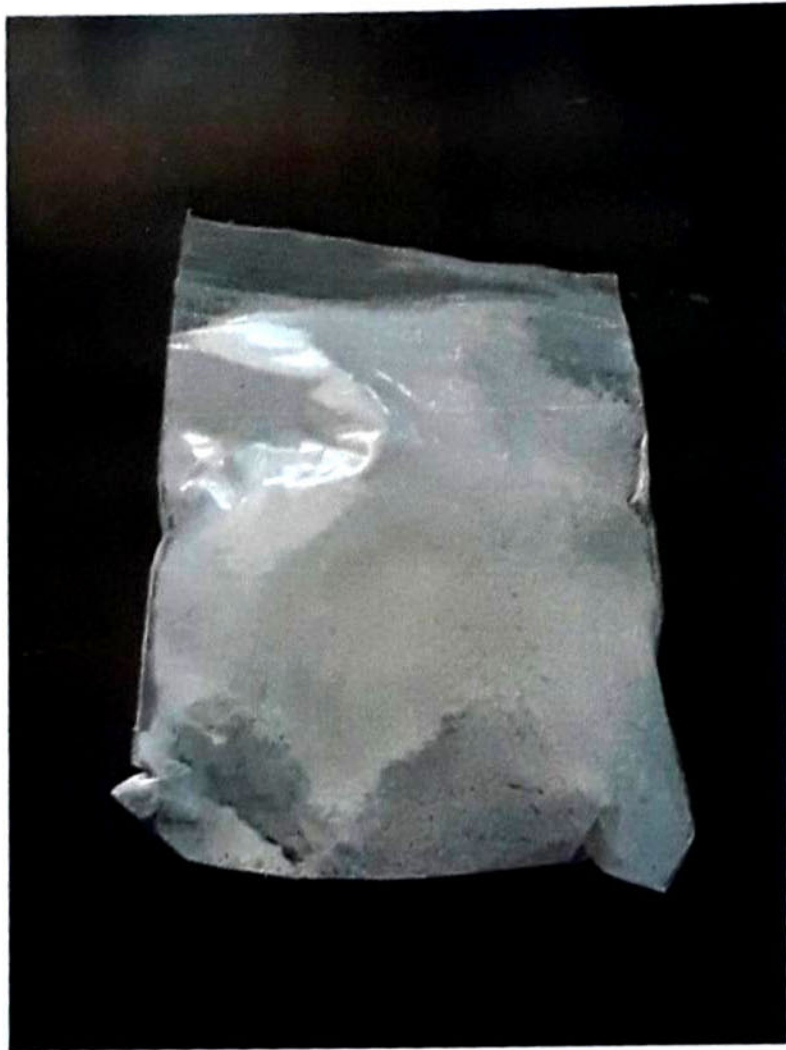


**Fig 2.1 (b) Titanium Dioxide**



**Fig 2.1 (a) Lead (II) Nitrate**



**Fig 2.1 (c) Potassium Hydroxide**

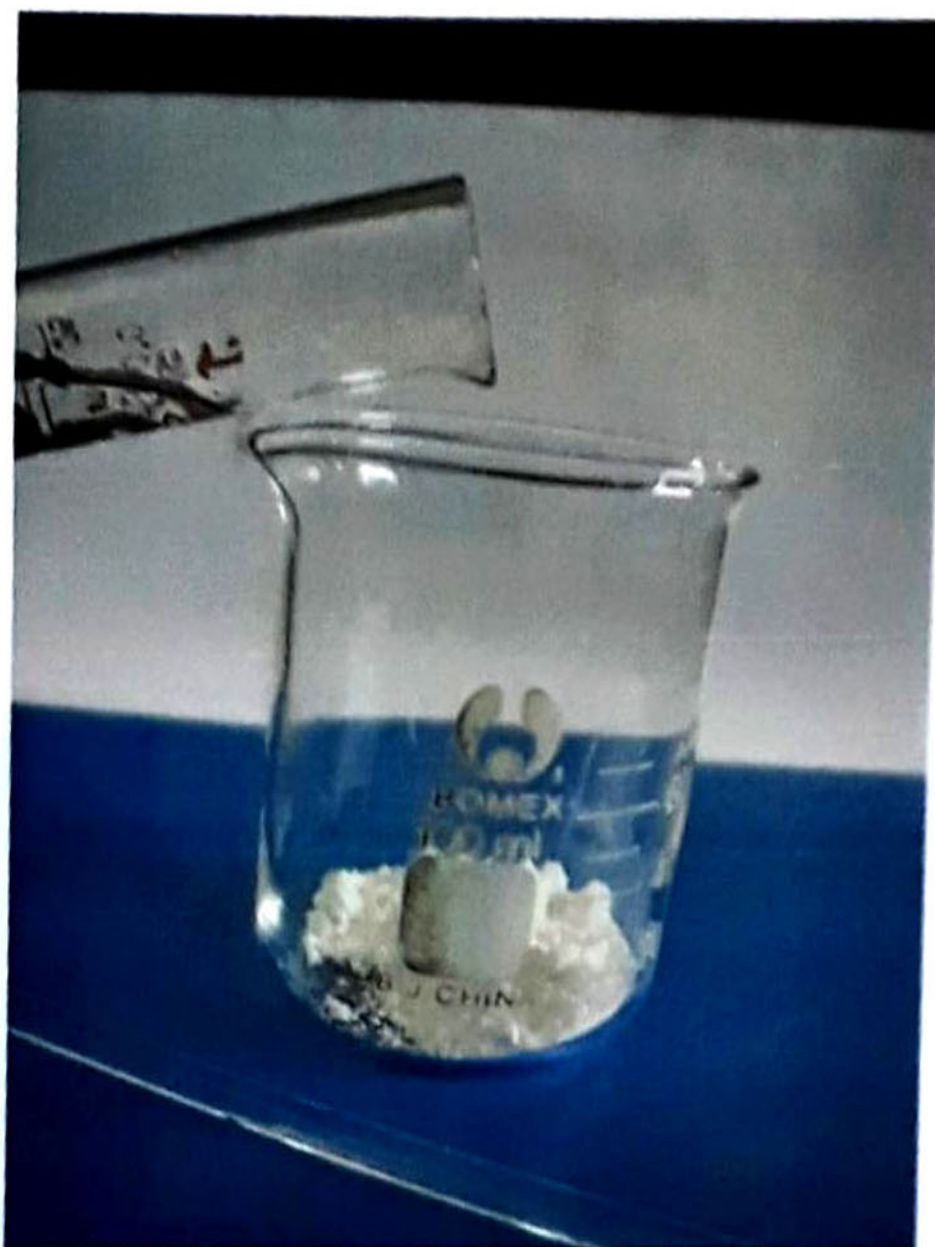


**Fig 2.2 (a) Mixing the Starting Reagents**

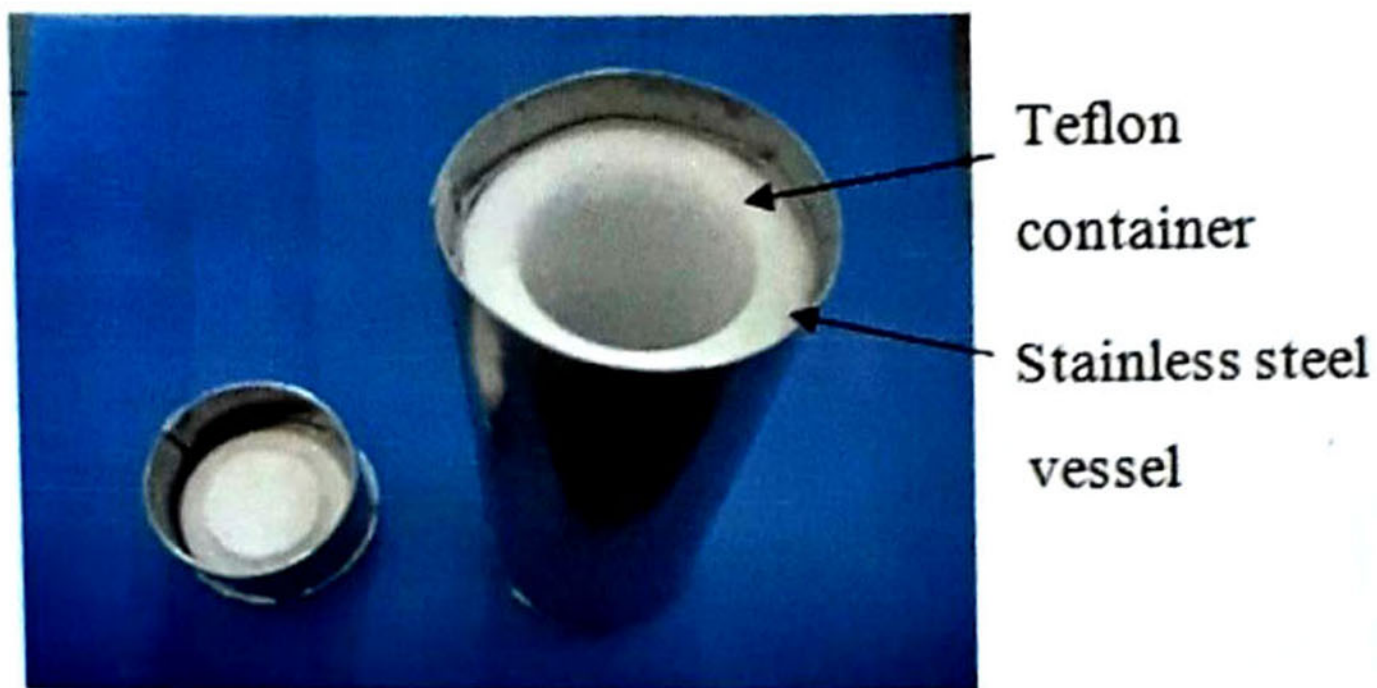


**Fig 2.1 (d) Teflon – lined Stainless Steel Bomb**

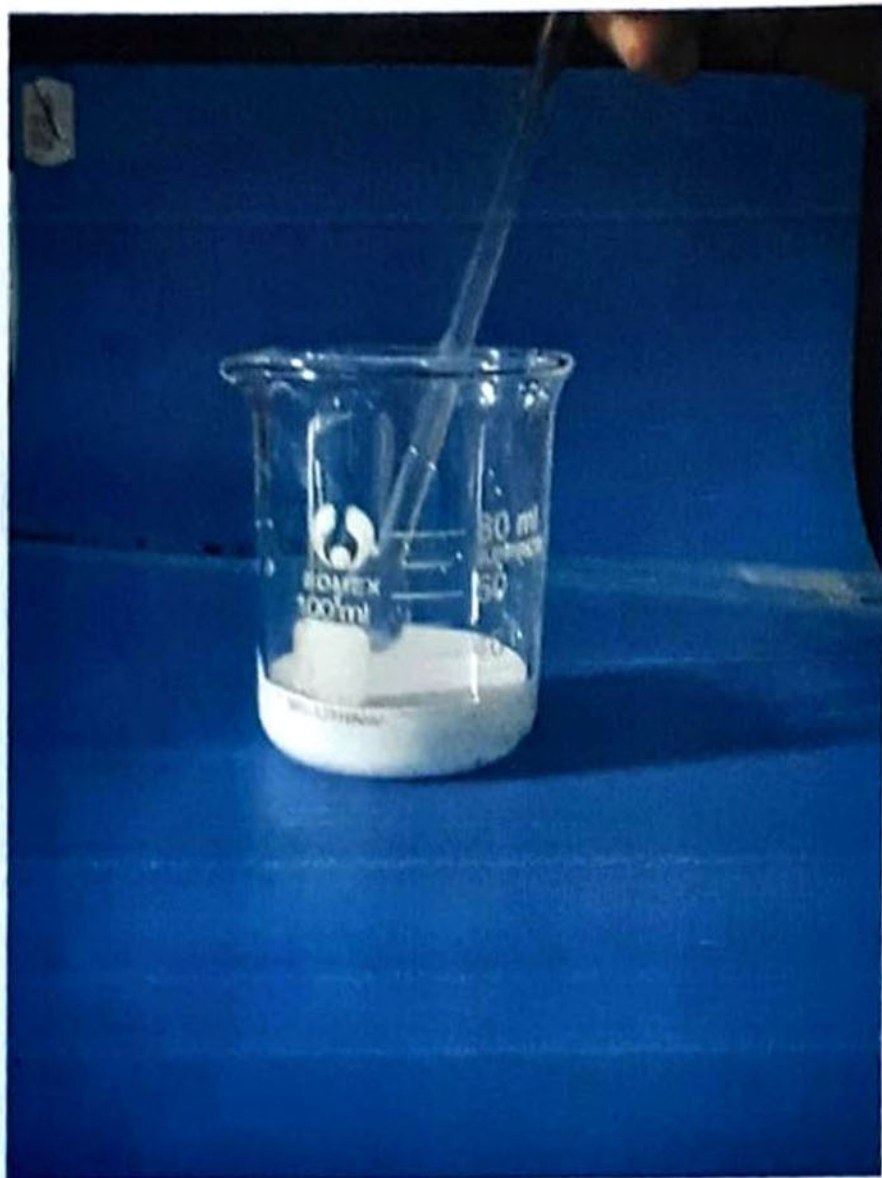


**Fig 2.2 (b) Stir with Glass Rod**

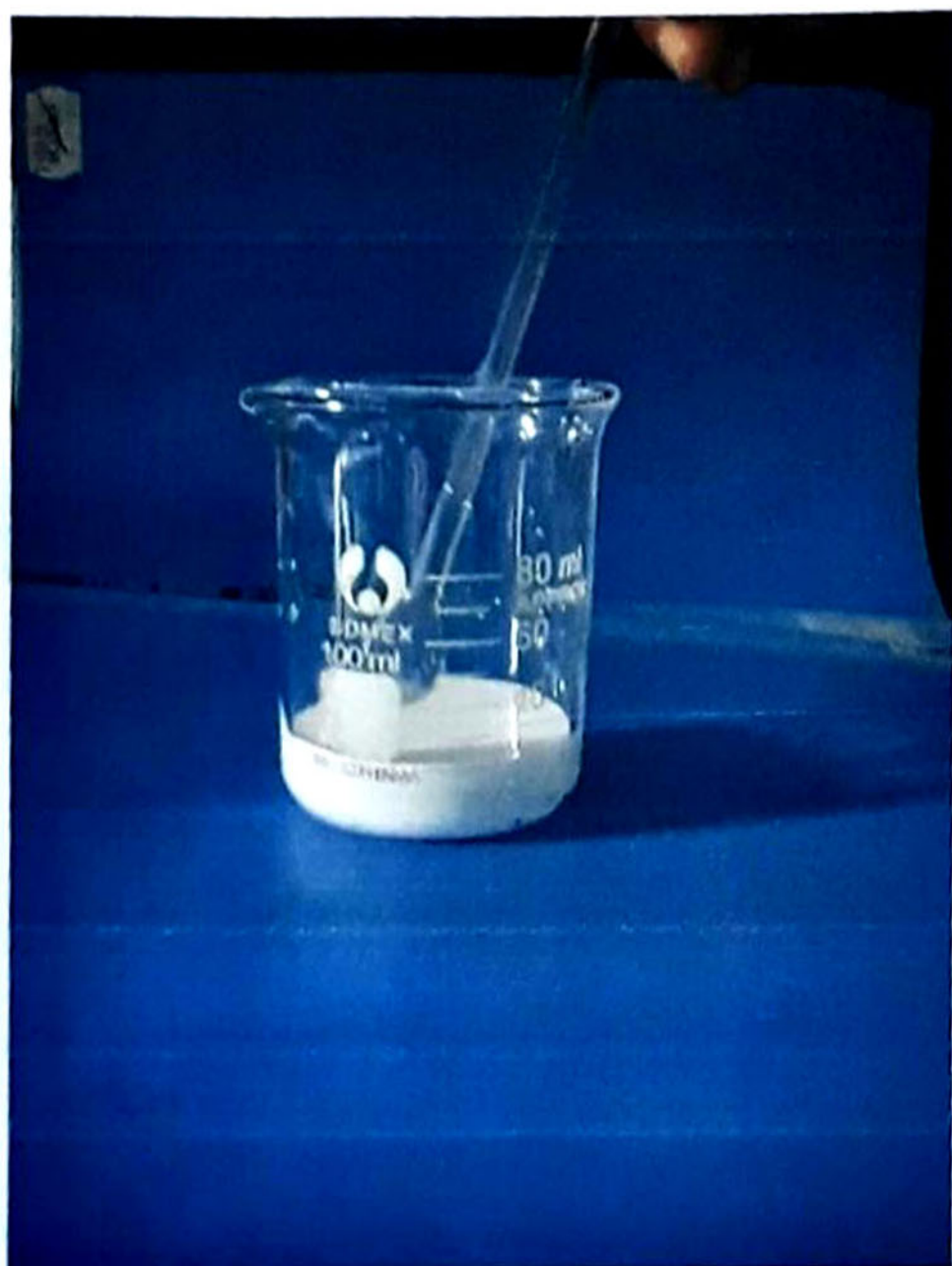


**Fig 2.2 (b) Stir with Glass Rod**



**Fig 2.2 (b) Stir with Glass Rod**



**Fig 2.2 (c) Pour Mix Solution into Stainless Steel Bomb**



**Fig 2.3 (a) Same Colour of  $\text{PbTiO}_3$  Powders**



**Fig 2.2 (d) Hydrothermal Bath**

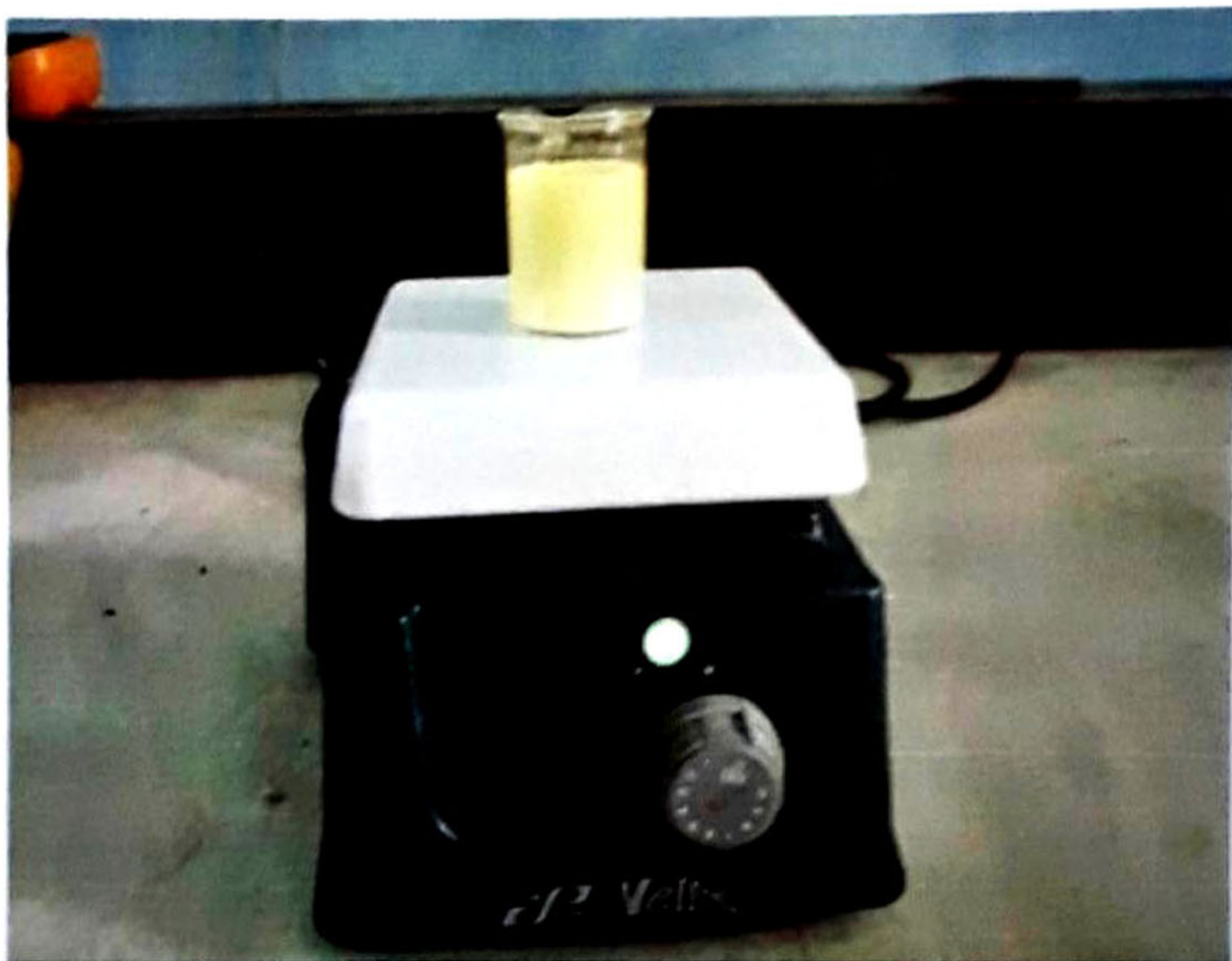


**Fig 2.3 (b) The Magnetic Stirrer**



**Fig 2.3 (d) Single Wafer Spin Processor**

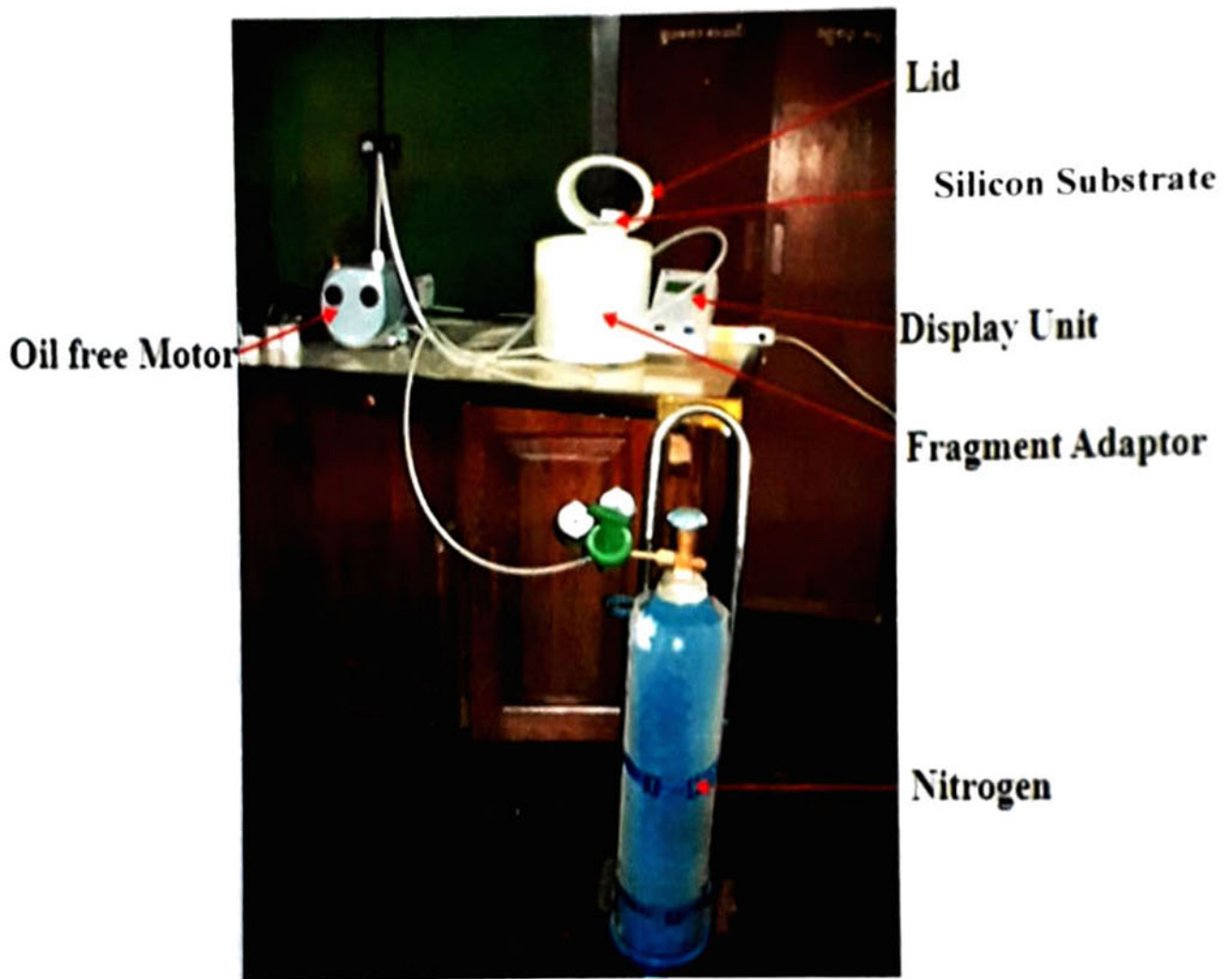


**Fig 2.3 (c) The Photograph of Spin Coating System of the Spin Processor (MODEL WS-400BZ- 6N PP/LITE)**

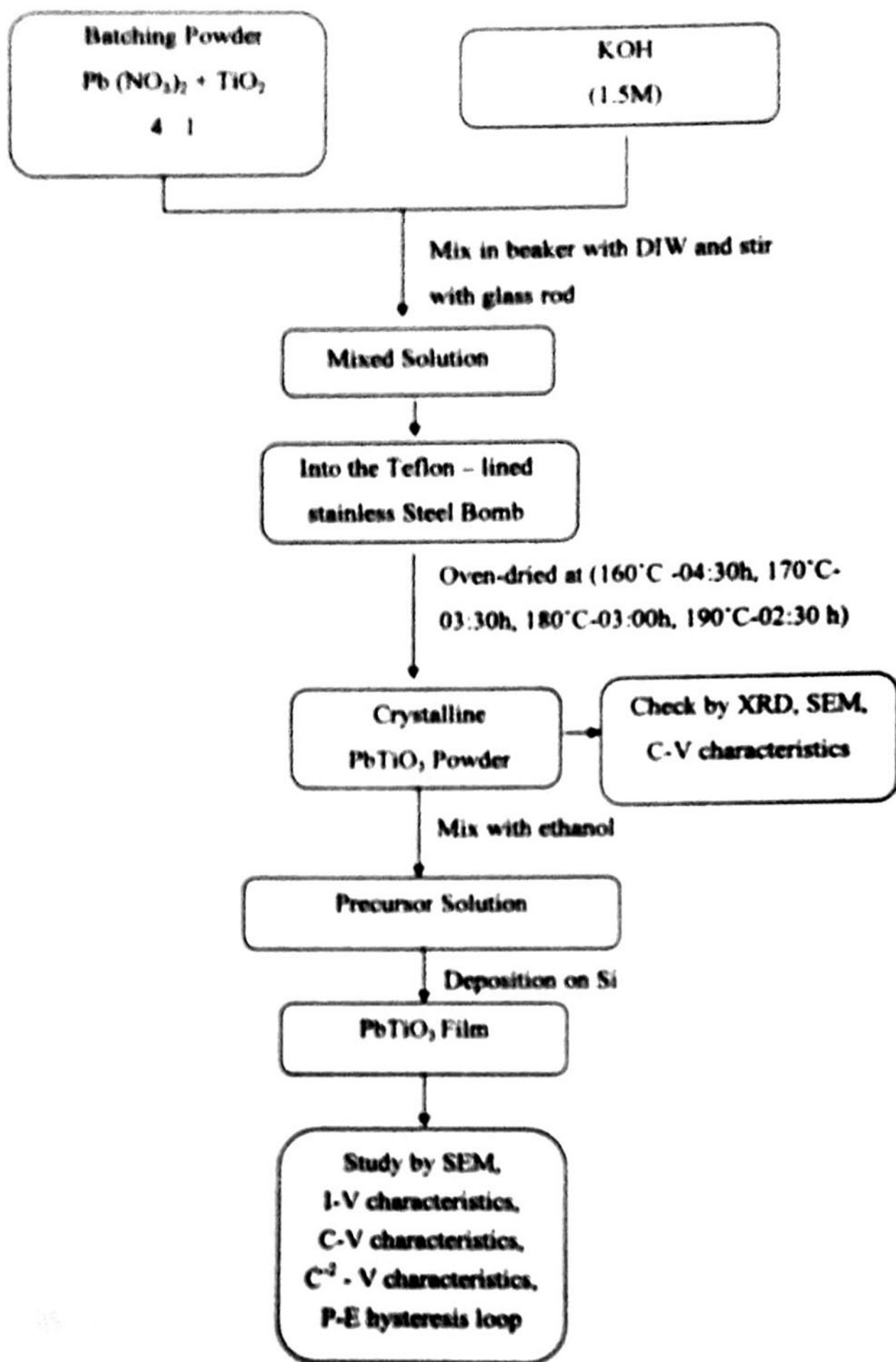


**Fig 2.4 Experimental Procedure**

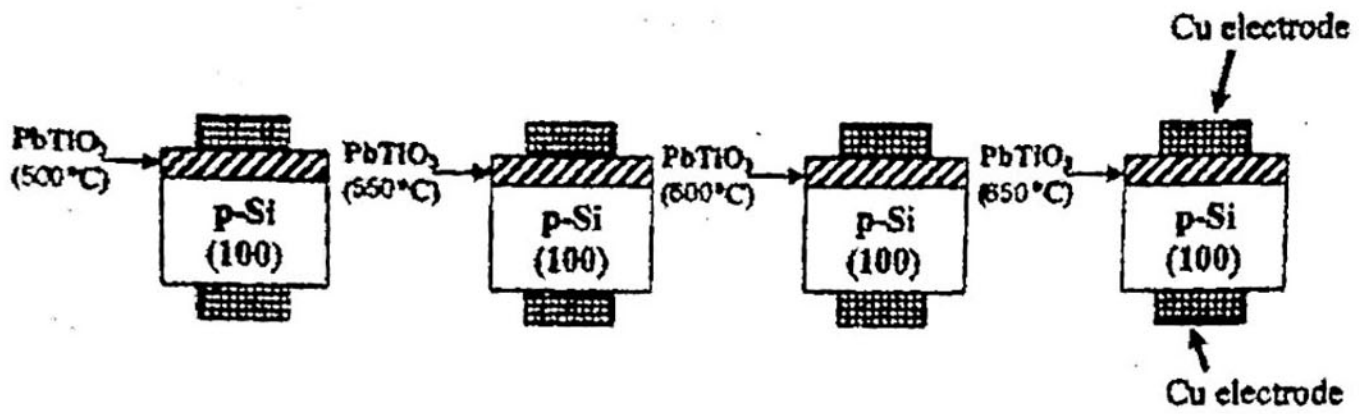


Fig 2.3 (e) The  $\text{PbTiO}_3/\text{p-Si}$  Structure Process Temperature

The lattice strain / lattice microstrain (c/a) was also shown in Table 3.2.

**Table 3.2 Lattice Strain / Tetragonality of both Values**

Annealing Temperature (°C)	Tetragonality c/a	
	Standard	Observed
160	1.082283	1.062964
170	1.082283	1.0573457
180	1.082283	1.0604743
190	1.082283	1.0582804

### 3.1.2 Crystallite Size (Nano-Particle size)

The crystallite size was evaluated by eqn:

$$\text{Crystallite size} = \frac{0.899 \times \lambda(\text{\AA})}{\text{FWHM}(\text{rad}) \times \cos\theta_B} \dots\dots\dots(4.2)$$

Where  $\lambda$  = 1.54056 Å for Cu  $k_{\alpha}$  relation

FWHM = full width at half maximum value for (101) diffracted peak

$\theta_B$  = value of  $\theta$  for (101) diffracted peak

The crystallite size (nano-particle size) was collected and listed in Table 3.3.

**Table 3.3 Crystallite Size at Different Annealing Temperatures**

Annealing Temperature (°C)	Crystallite Size (nm)
160	32.6
170	34.4
180	28.6
190	44.3

### 3.2 Microstructural Study by SEM

The morphologies of the resulting hydrothermal PbTiO<sub>3</sub> powders were studied by Scanning Electron Microscope (SEM). SEM images for PbTiO<sub>3</sub> powders at 160°C, 170°C, 180°C and 190°C were described at Fig 3.2 (a-d). It was found that randomly oriented samples on SEM images were formed. All images

showed the fairly dense structures with fine grains and without cracks. The grain sizes were measured to be 32.08 $\mu\text{m}$ , 33.00 $\mu\text{m}$ , 35.00 $\mu\text{m}$ , and 33.75 $\mu\text{m}$  for respective powders. The grain orientation was also left-shifted. In addition it was well known that the hydrothermal synthesized  $\text{PbTiO}_3$  powder was quite feasible for ceramic growth technology. From SEM results, it was seemed that the  $\text{PbTiO}_3$  powder was fine and successfully grown. The best powder was appeared at reaction temperature of 190°C.

### 3.3 C-V Characteristics of Lead Titanate Ceramic Capacitor

Fig 3.3 (a-d) indicated the capacitance and voltage characteristics of ceramic capacitor. Measurement was performed at 100 kHz and dc bias voltage cycled at  $\pm 5\text{V}$ . The C-V curve gave the nonvolatile behaviour and also indicated the memory function. The hysteresis gap showed the width of memory window and it was measured to be 0.42 V, 0.41 V, 0.63, 0.64 V, respectively.

### 3.4 Morphology and Film Thickness by SEM

Fig 3.4 (a-d) showed the SEM image (planner view) of  $\text{PbTiO}_3$  film. The grain was uniformly distributed on SEM image for all samples. The grain size was measure by well-know bar code system. They were 2.2  $\mu\text{m}$ , 1.65  $\mu\text{m}$ , 1.05  $\mu\text{m}$  and 0.8  $\mu\text{m}$  for respective films. From SEM Photomicrograph, it was obvious that the altering solution chemistry was quite acceptable and appropriate for growth mechanism. Fig 3.4 (e-h) showed the SEM image (cross-sectional view) of  $\text{PbTiO}_3$  film. The film thickness were found to be 27.8  $\mu\text{m}$ , 28.6  $\mu\text{m}$ , 23.7  $\mu\text{m}$  and 24.5  $\mu\text{m}$  respectively.

### 3.5 I-V Characteristics of $\text{PbTiO}_3$ Films

Electrical properties of  $\text{PbTiO}_3$  films were interperal by means of I-V characteristics. Fig 3.5 (a) showed the I-V characteristics of  $\text{PbTiO}_3$  films at different process temperatures. This curve showed the rectification effect because the forward and reverse regions were asymmetric.  $\ln|I-V$  variation was

## CHAPTER III

### RESULTS AND DISCUSSION

#### 3.1 Phase Formation of PbTiO<sub>3</sub> Powder

Lead titanate (PbTiO<sub>3</sub>) powders were thus obtained and examined their structural properties by X-ray Diffraction (XRD) technique. Fig 3.1 (a-d) indicated the XRD profiles of PbTiO<sub>3</sub> powders at different annealing temperatures. All observed XRD profiles were absolutely matched with those of standard PbTiO<sub>3</sub> peak with tetragonal symmetry. Thus PbTiO<sub>3</sub> specimen was successfully formed at given annealing temperatures. In this study the annealing temperature was limited from 160°C to 190°C. (101) diffracted peak was found to be rather sharp over others for all XRD profiles. However the (101) peak was appeared with co-existing peak named (110) reflection for all XRD plot except at 190°C. The intensity of XRD profile was largest for PbTiO<sub>3</sub> powder at 190°C while the smallest value was caused at 160°C.

##### 3.1.1 Lattice Parameters, Lattice Distortion and Cell Volume

The lattice parameters of PbTiO<sub>3</sub> powder for both standard and observed values at different annealing temperatures were listed in Table 3.1.

**Table 3.1 Lattice Parameters for both Standard and Observed Values**

Annealing Temperature (°C)	Lattice Parameters			
	a (Å)		c (Å)	
	Standard	Observed	Standard	Observed
160	3.889	3.8927	4.209	4.1378
170	3.889	3.9009	4.209	4.1246
180	3.889	3.8876	4.209	4.1227
190	3.889	3.8881	4.209	4.1147

film (at 500°C - 650°C) were examined by Quard Tech 1730 LCR Digibidge meter (Digital Impedence Analyzer) and DT 9208 digital multimeter as a voltmeter.

The  $C^{-2} - V$  characteristics of Lead titanate films were shown in Fig 3.7 (a-d). All  $C^{-2} - V$  graphs were linear relationships with different slopes. This fact gave the uniform and homogeneous Lead titanate specimen on substrate. From the graph, it was observed that the capacitance became saturating and independence of the bias voltage in excess 5 V because these depletive region have reached the end of n-Zone. At the point, the capacitance was of the order of  $10^{-13} (F)^{-2}$ . By extrapolating the linear graph, built - in - potential ( $V_{bi}$ ) was obtained. The value of  $V_{bi}$  lied in the positive region. This fact indicated the P-type conductivity of Si substrate. It also shown these n-side was at the higher potential than p-side. Acceptor concentration ( $N_a$ ), and repletion layer with ( $W$ ) were measured.

The built-in-potential, acceptor concentration and depletion layer width were listed in Table 3.6.

**Table 3.6 The Relationship of Reaction Temperature and  $N_a$ ,  $W$  and  $V_{bi}$**

Reaction Temperature (°C)	$N_a$ (cm <sup>-3</sup> )	$W$ (cm)	$V_{bi}$ (V)
500	$1.31 \times 10^{26}$	$1.04 \times 10^{-9}$	$3.50 \times 10^{-1}$
550	$6.68 \times 10^{25}$	$9.75 \times 10^{-10}$	$3.75 \times 10^{-1}$
600	$8.24 \times 10^{25}$	$1.00 \times 10^{-9}$	$3.38 \times 10^{-1}$
650	$8.24 \times 10^{25}$	$1.00 \times 10^{-9}$	$3.36 \times 10^{-1}$

### 3.8 P-E Hysteresis Loop Measurement

Thermal hysteresis loop was measured by Sawyer-Tower circuit. The observed hysteresis loops were given as Fig 3.8 (a-d). All hysteresis loops observed in present investigation were non-saturating as could be seen in figure. Further increase of electric field in the film caused its breakdown. Especially, the loop formed at 500°C [Fig 3.8 (a)] was examined to be round-ended. All loops were

non-linear and tended to ferroelectric behaviour. It was clearly found that the fabricated  $\text{PbTiO}_3$  film exhibited the ferroelectric properties. The three hysteresis parameters such as spontaneous polarization density ( $p_s$ ), remanent polarization density ( $P_r$ ) and coercive field ( $E_c$ ) were measured. The reference capacitance and resistance used in this study were  $1.4 \times 10^{-11} \text{F}$  and  $330 \text{k}\Omega$ .

From the view point of digital electronic, the fabricated  $\text{PbTiO}_3$  films can be used as a prototype device of non-volatile memory application. Fig 3.9 (a) showed the change in  $2P_r$  (Polarization reversal) as a function of process temperatures. The largest value was found at  $600^\circ\text{C}$ . Fig 3.9 (b) indicated the variation of  $P_s$  and process temperatures. The nature of  $P_s$ -T was examined to be same as that of  $2P_r$ -T. The variation of  $E_c$  with respect to process temperature was shown in Fig 3.9 (c). These value were also described at Table 3.7.

shown in Fig 3.5 (b). The diode quality factor (ideality factor)( $\eta$ ) and zero-bias barrier height ( $\Phi_{bo}$ ) were described in Table 3.4.

**Table 3.4 Some Diode Parameters of PbTiO<sub>3</sub> Films at Different Process Temperatures**

Temp(°C )	$\Phi_{bo}$ (eV)	$\eta$
500	0.516740	0.9850
550	0.529851	1.6117
600	0.527653	1.2654
650	0.530886	1.2837

### 3.6 C-V Characteristics of PbTiO<sub>3</sub> Films (Nonvolatile Memory Nature)

To examine the ferroelectric memory nature of hydrothermal synthesized PbTiO<sub>3</sub> film, capacitance and voltage characteristics was measured at 100 kHz. The double sweeping voltage was applied from -5V to +5V. Fig 3.6 ( a-d) gave the C-V characteristics of PbTiO<sub>3</sub> films at different process temperatures. The C-V curve exhibited the hysteresis nature as well as memory behaviour. Table 3.5 described the change in memory window with respect to process temperature.

**Table 3.5 Width of Memory Window at Different Process Temperatures**

Temp(°C )	Memory window (V)
500	0.60
550	0.53
600	0.26
650	0.27

### 3.7 C<sup>2</sup>-V Characteristics of Lead Titanate Film

Charge conduction mechanism ( $1/C^2$ -V) of PbTiO<sub>3</sub>/p-Si at process temperature were studied. C-V Characteristics of hydrothermal derived PbTiO<sub>3</sub> ceramic

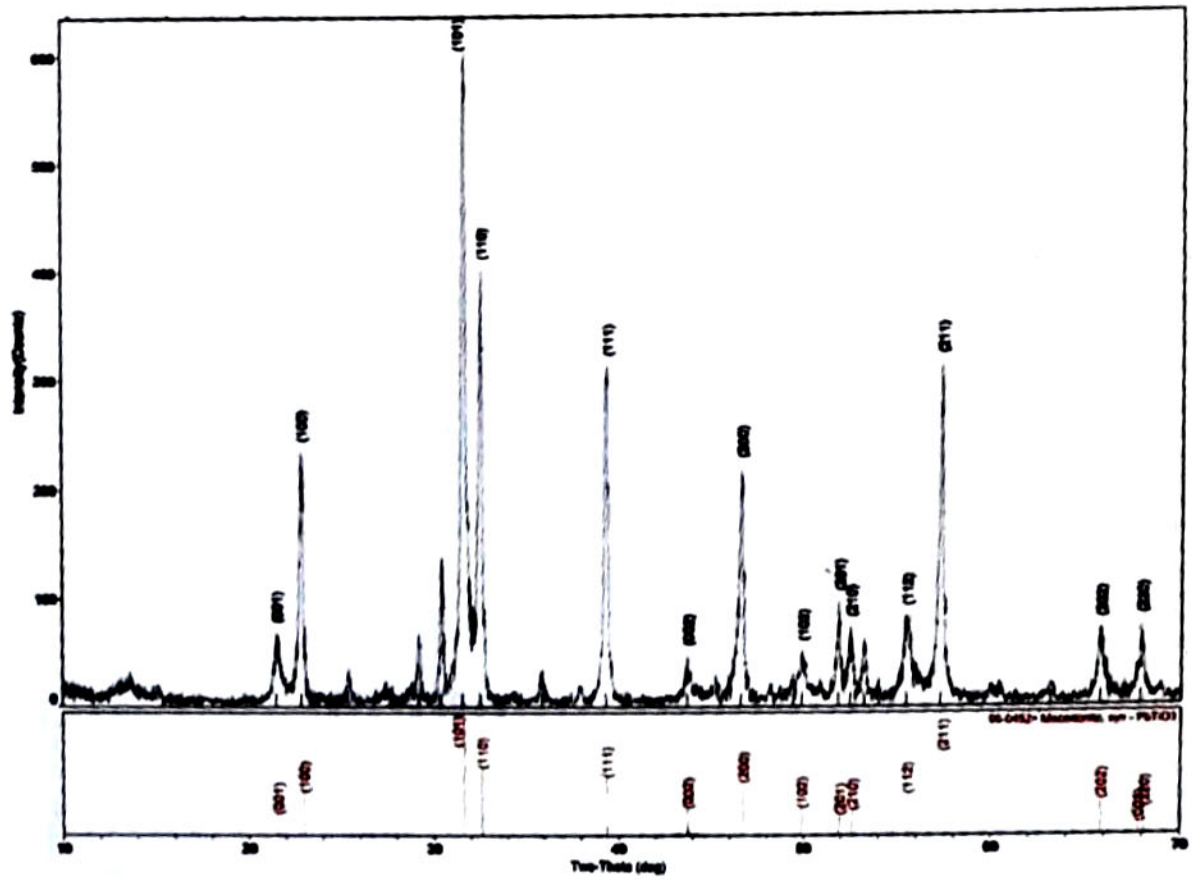


Fig 3.1 (a) XRD Profile for PbTiO<sub>3</sub> Powder at 160°C

**Table 3.7 P<sub>r</sub>, P<sub>s</sub> and E<sub>c</sub> Different Temperature**

Process Temp (°C)	C (F)	Area (cm <sup>2</sup> )	Thickness (m)	x-axis 0.1 (V)	y-axis 0.1 (V)	2P <sub>r</sub> (C/cm <sup>2</sup> )	P <sub>s</sub> (C/cm <sup>2</sup> )	E <sub>c</sub> (V/m)	2P <sub>r</sub> (μC/cm <sup>2</sup> )	P <sub>r</sub> (μC/cm <sup>2</sup> )	P <sub>s</sub> (μC/cm <sup>2</sup> )	E <sub>c</sub> (KV/cm)
500	1.40E-11	7.86E-05	2.16E-03	0.4	0.002	5.70E-07	2.67E-09	1.02E+03	5.70E-01	2.85E-01	2.67E-03	1.02E+00
550	1.40E-11	7.86E-05	2.16E-03	0.4	0.002	7.13E-07	3.21E-09	9.26E+02	7.13E-01	3.57E-01	3.21E-03	9.26E+00
600	1.40E-11	7.86E-05	2.16E-03	0.4	0.002	1.14E-06	5.70E-09	1.48E+03	1.14E-00	5.70E-01	5.70E-03	1.48E+01
650	1.40E-11	7.86E-05	2.16E-03	0.4	0.002	7.13E-07	3.56E-09	1.20E+03	7.13E-01	3.57E-01	3.56E-03	1.20E+01

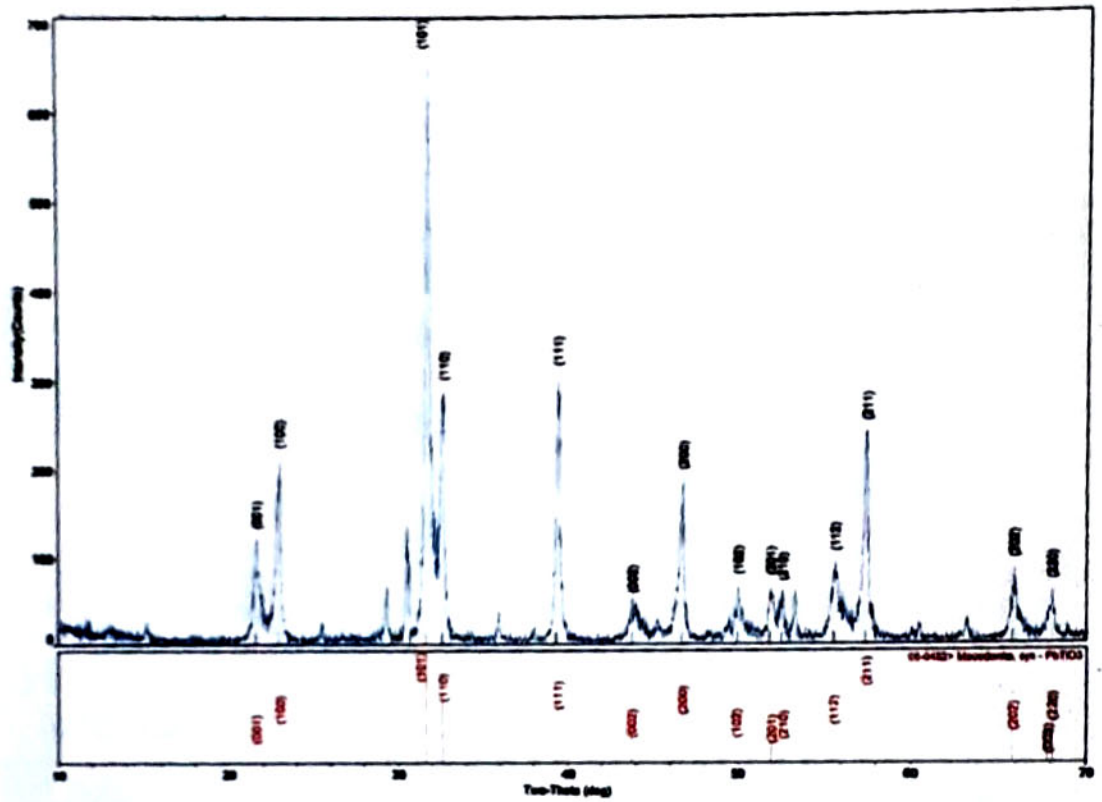


Fig 3.1 (c) XRD Profile for PbTiO<sub>3</sub> Powder at 180°C

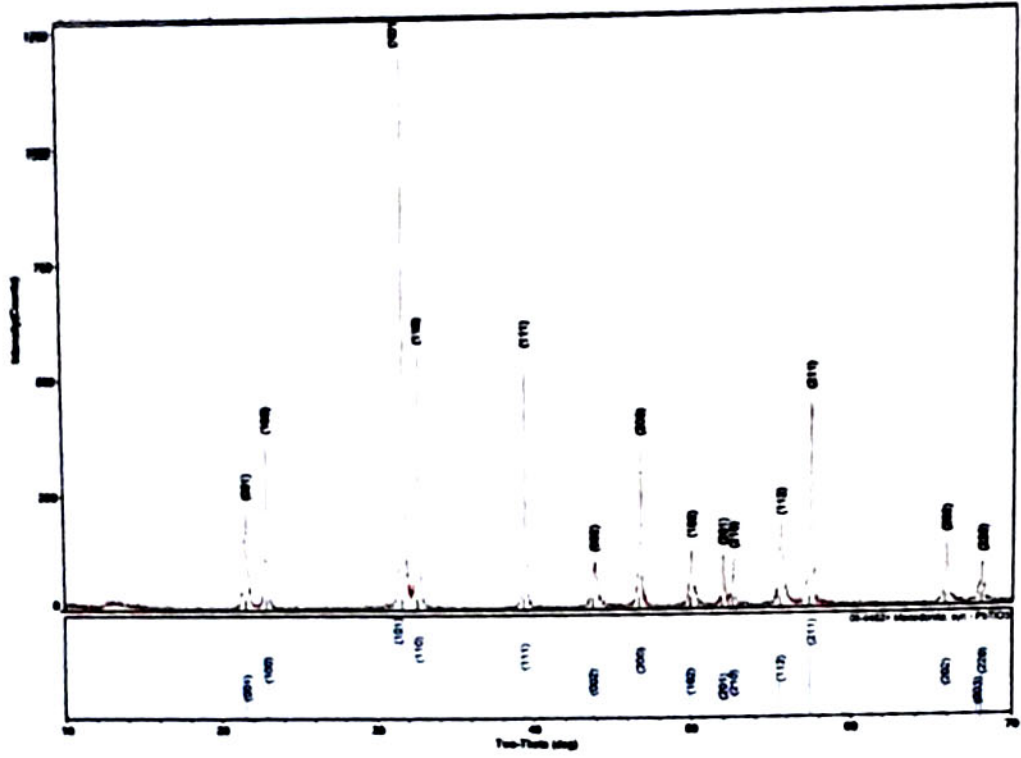


Fig 3.1 (d) XRD Profile for PbTiO<sub>3</sub> Powder at 190°C

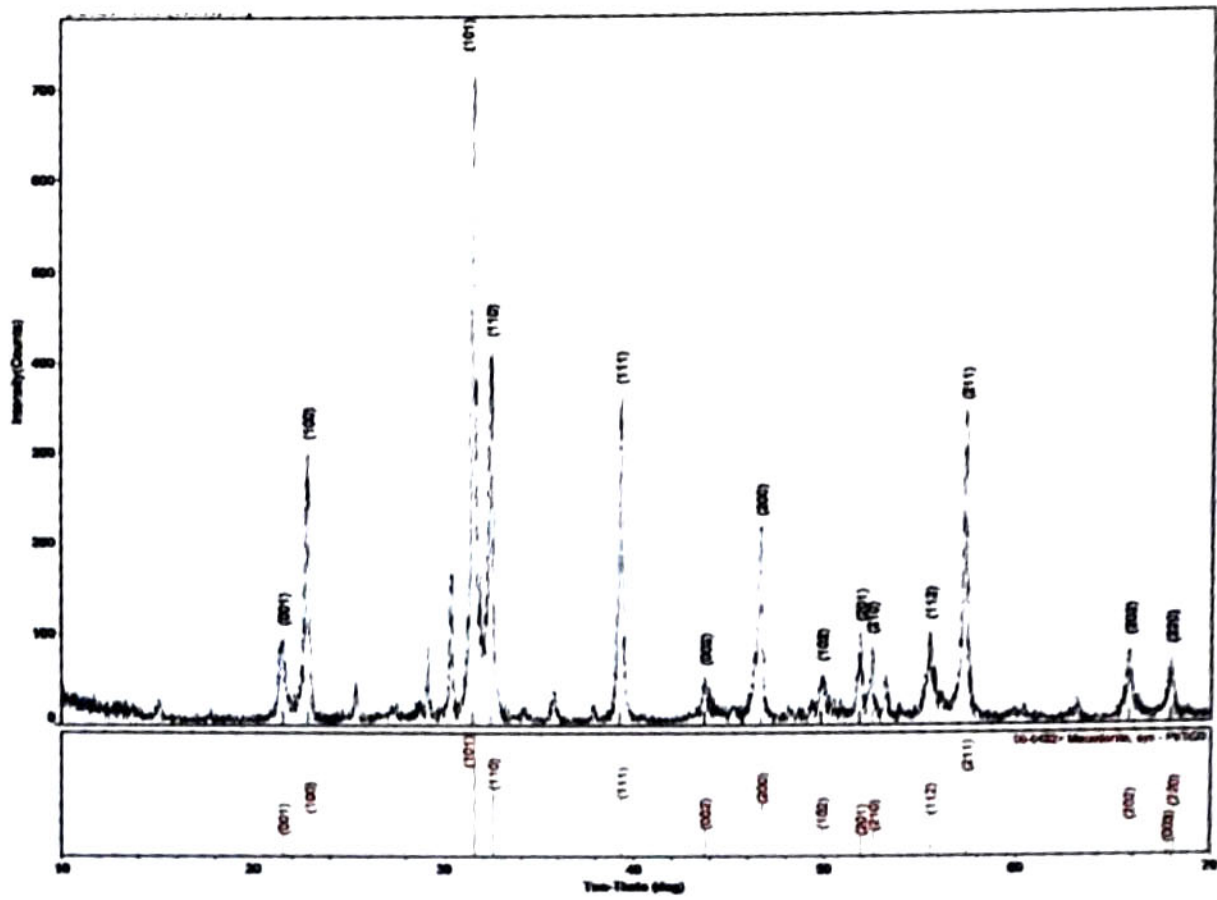
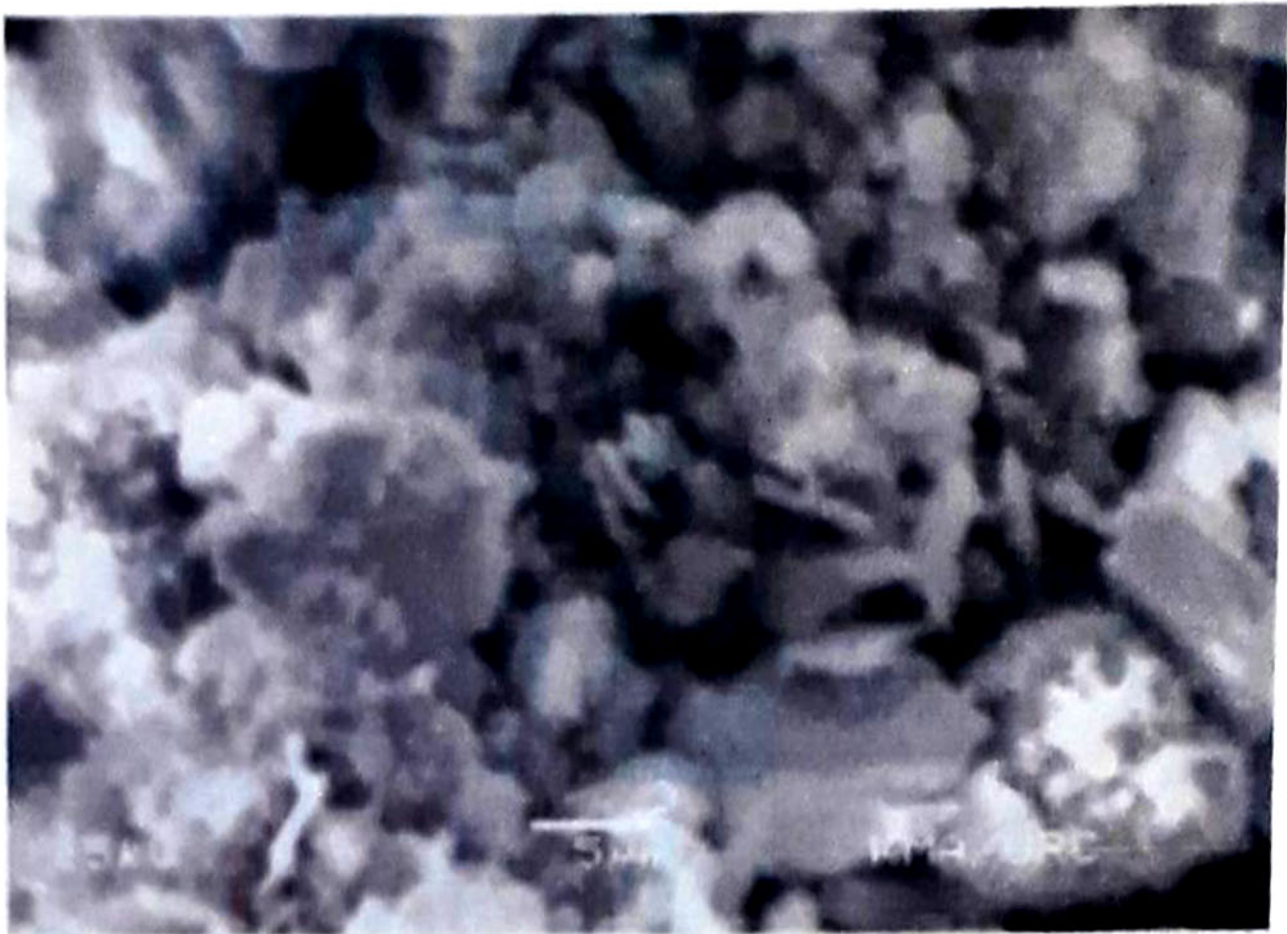
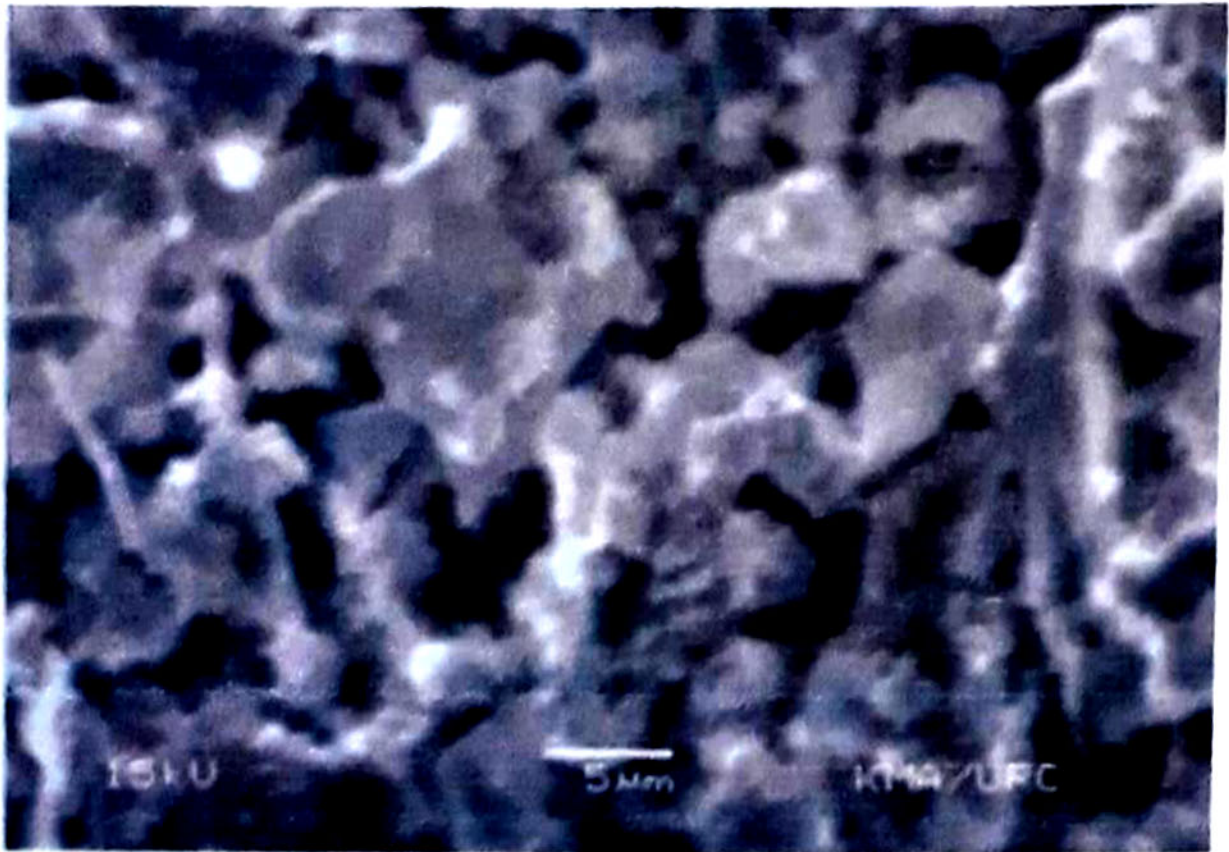


Fig 3.1 (b) XRD Profile for PbTiO<sub>3</sub> Powder at 170°C



**Fig 3.2 (b) SEM Image for PbTiO<sub>3</sub> Powder at 170°C**



**Fig 3.2 (a)** SEM Image for PbTiO<sub>3</sub> Powder at 160°C

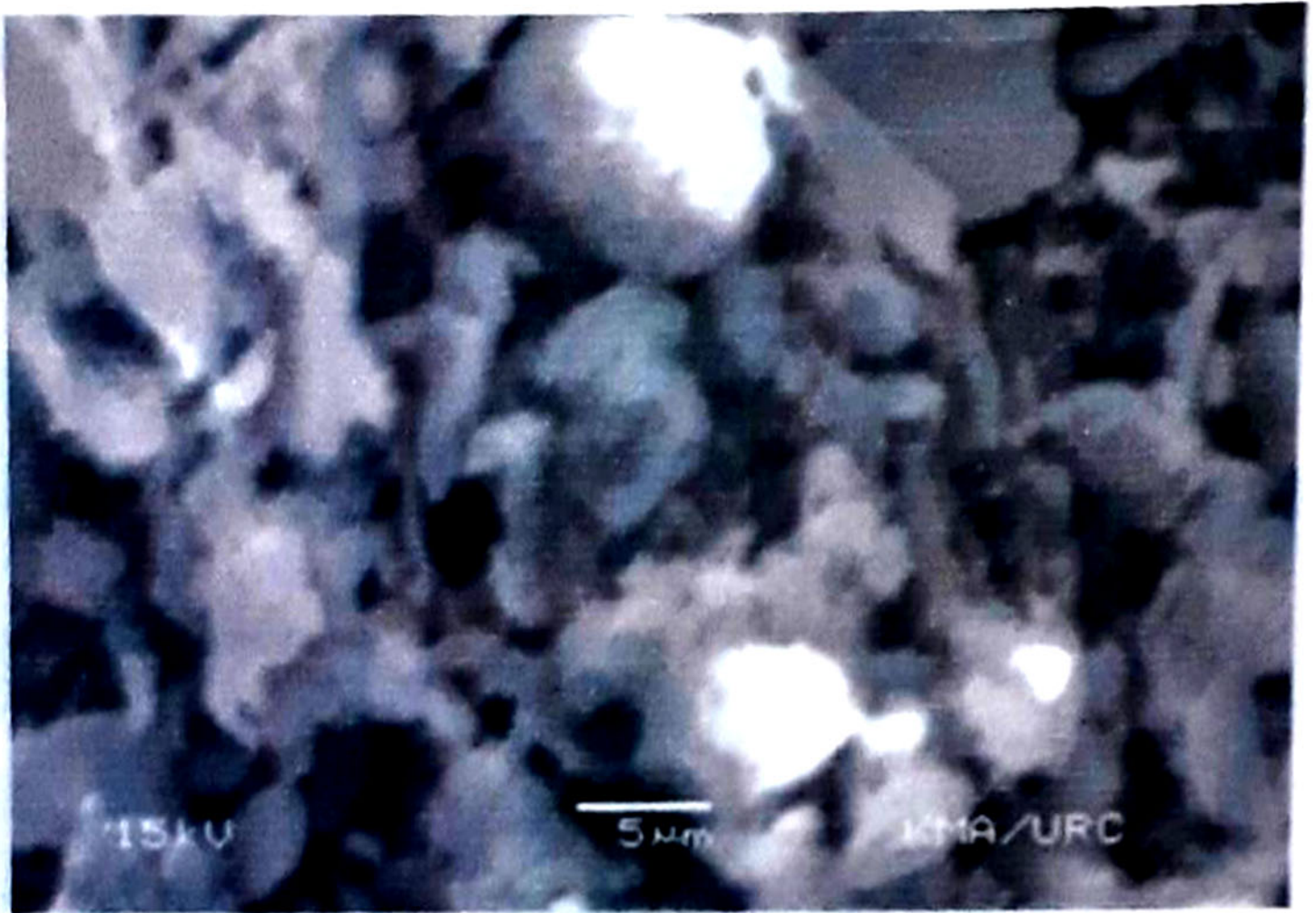


**Fig 3.2 (c) SEM Image for PbTiO<sub>3</sub> Powder at 180°C**

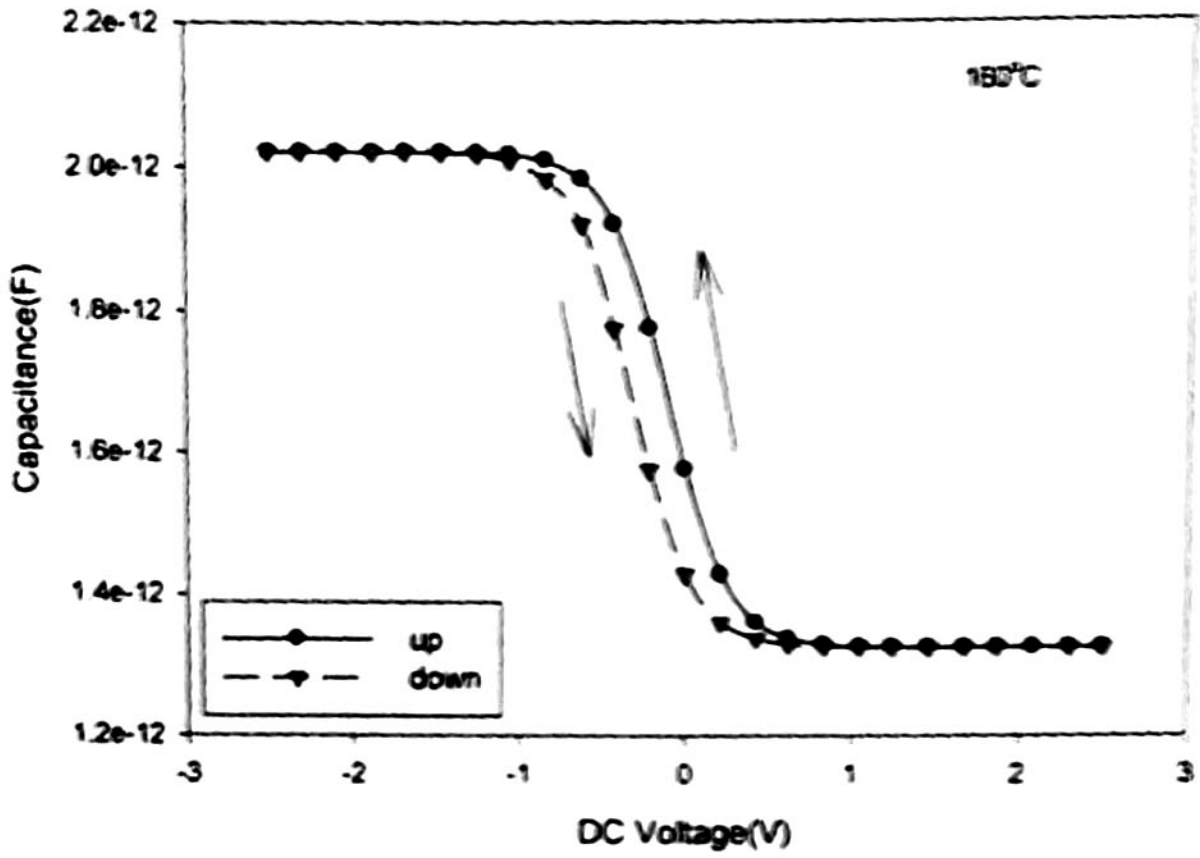


**Fig 3.3 (a) C-V Characteristics of PbTiO<sub>3</sub> Ceramic at 160°C**

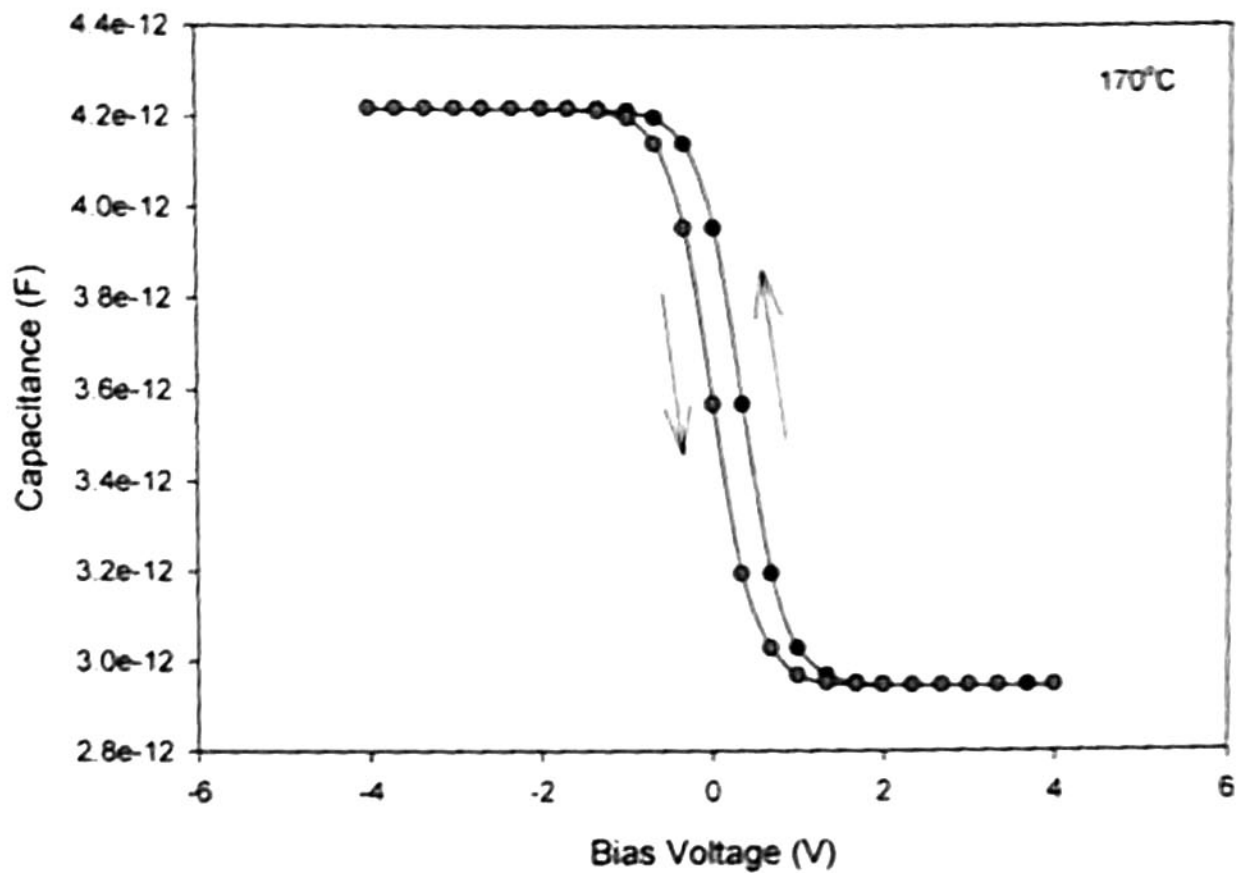


**Fig 3.3 (b) C-V Characteristics of PbTiO<sub>3</sub> Ceramic at 170°C**

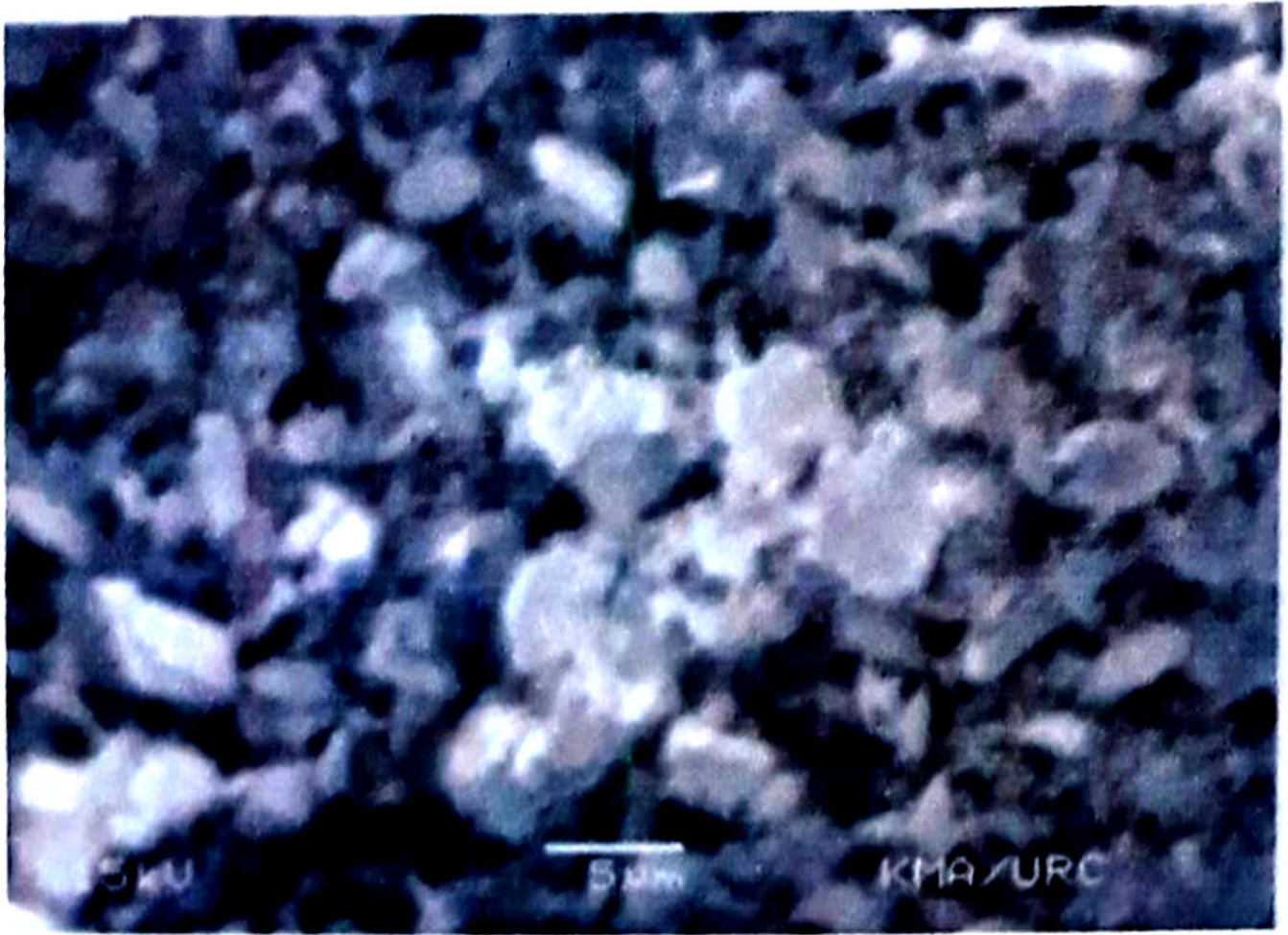


**Fig 3.2 (d) SEM Image for PbTiO<sub>3</sub> Powder at 190°C**

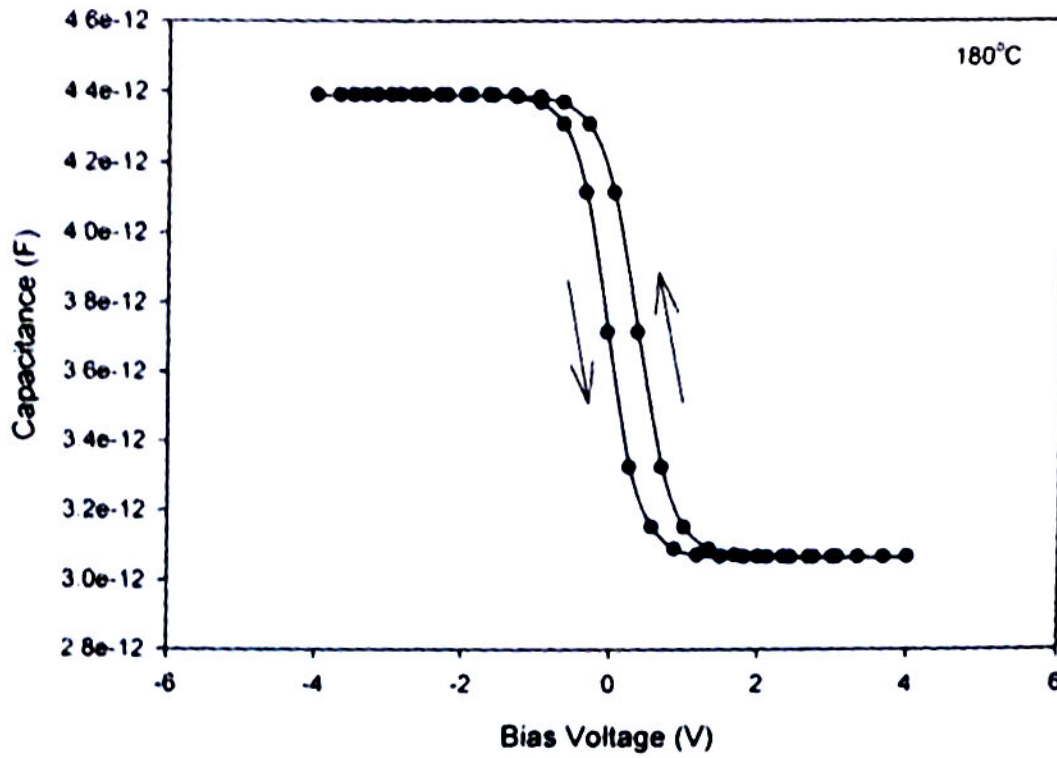


**Fig 3.3 (c) C-V Characteristics of PbTiO<sub>3</sub> Ceramic at 180°C**

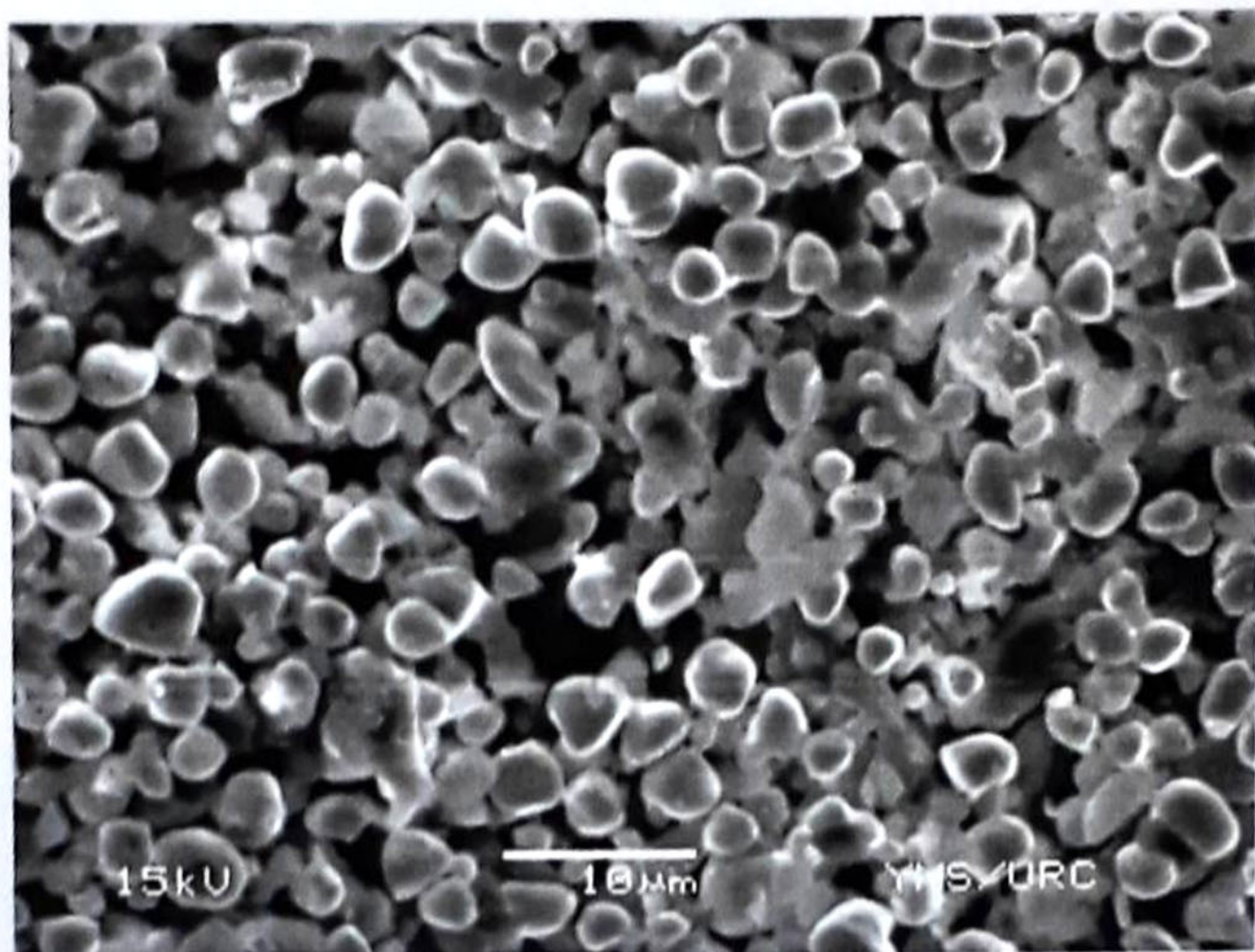


**Fig 3.4 (a)** SEM Image for PbTiO<sub>3</sub> Film at 500°C

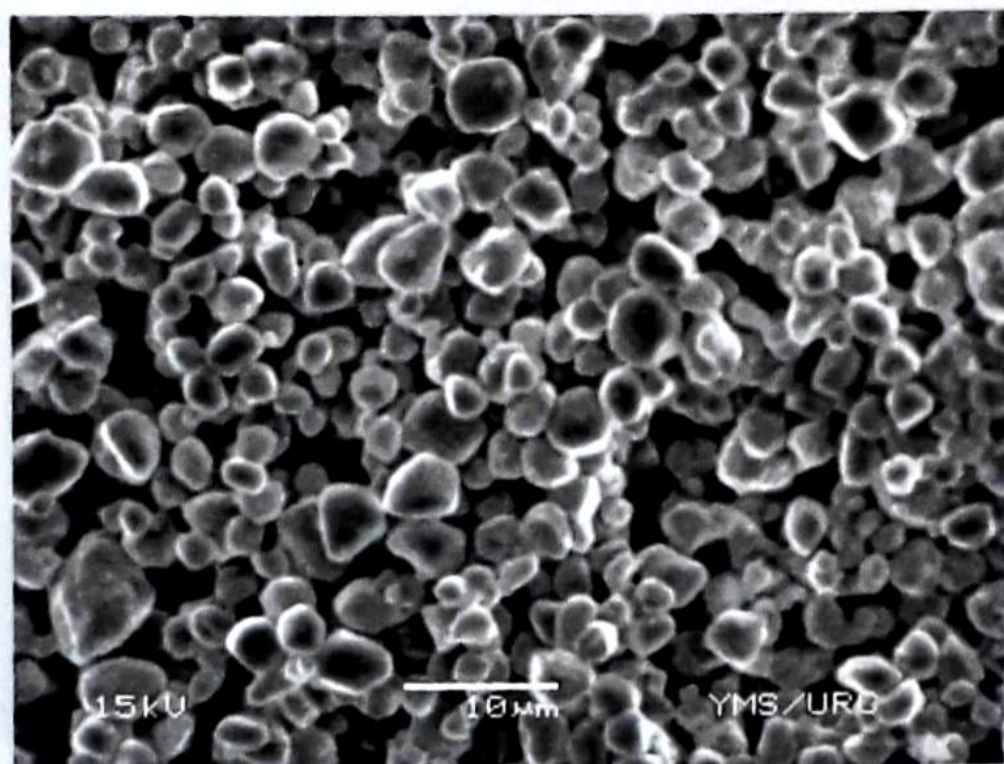


**Fig 3.4 (b)** SEM Image for PbTiO<sub>3</sub> Film at 550°C

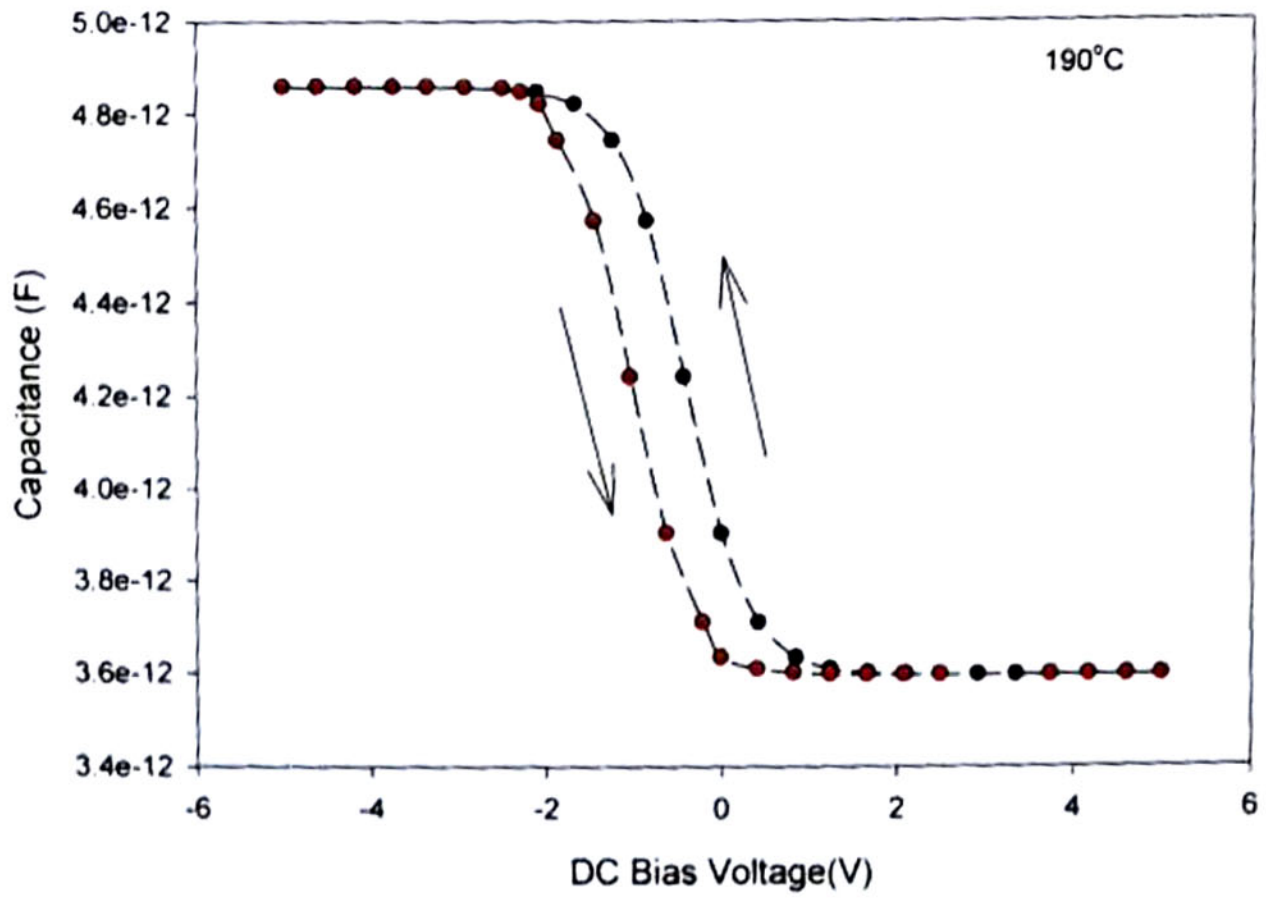


**Fig 3.3 (d) C-V Characteristics of PbTiO<sub>3</sub> Ceramic at 190°C**

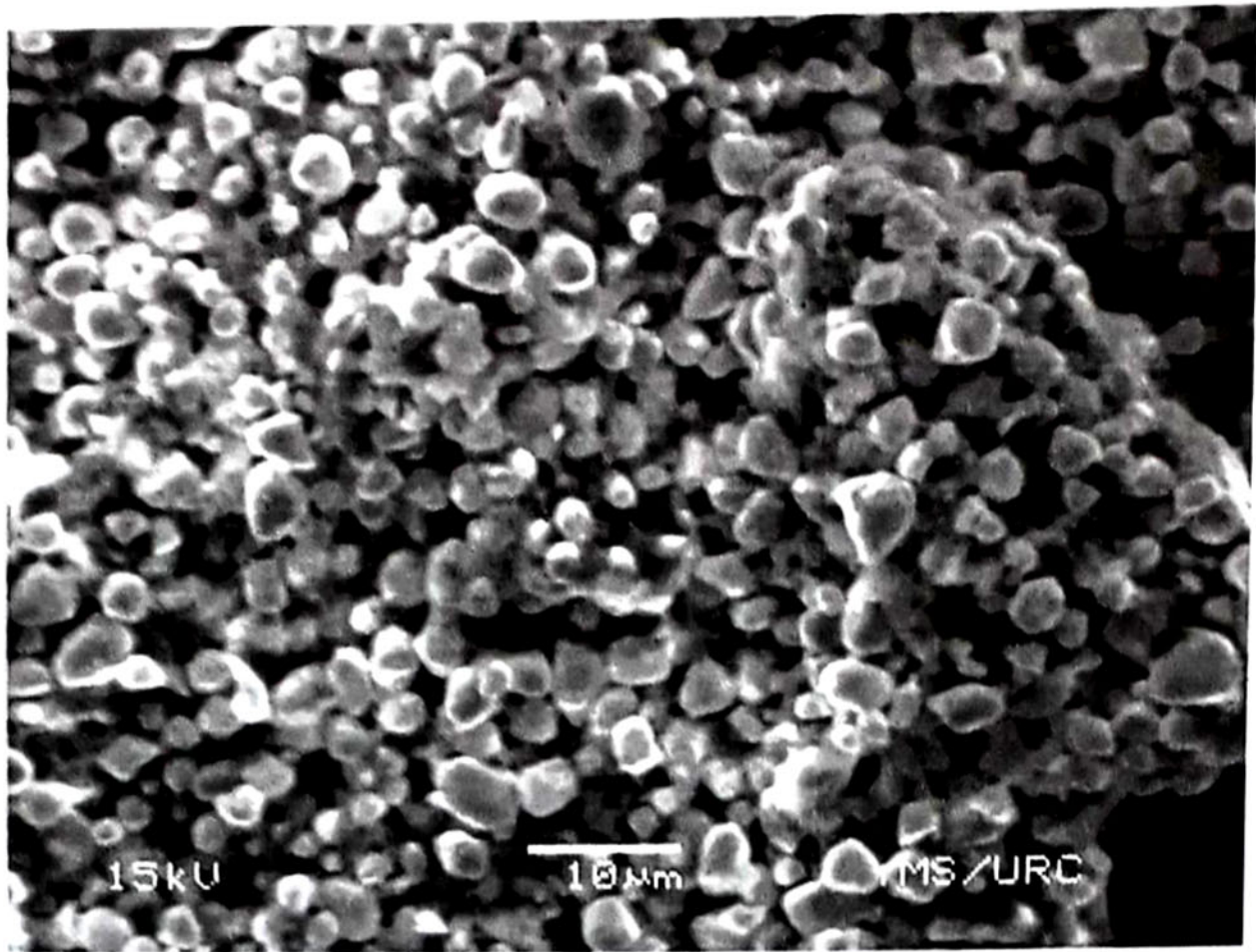


**Fig 3.4 (d) SEM Image for PbTiO<sub>3</sub> Film at 650°C**

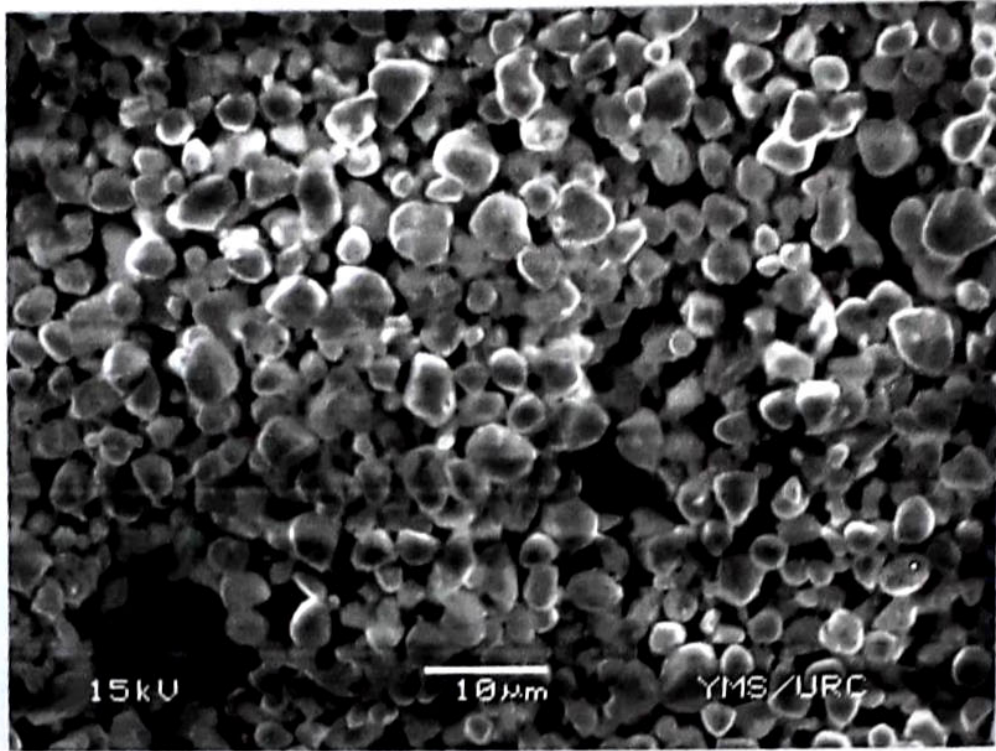


**Fig 3.4 (c) SEM Image for PbTiO<sub>3</sub> Film at 600°C**

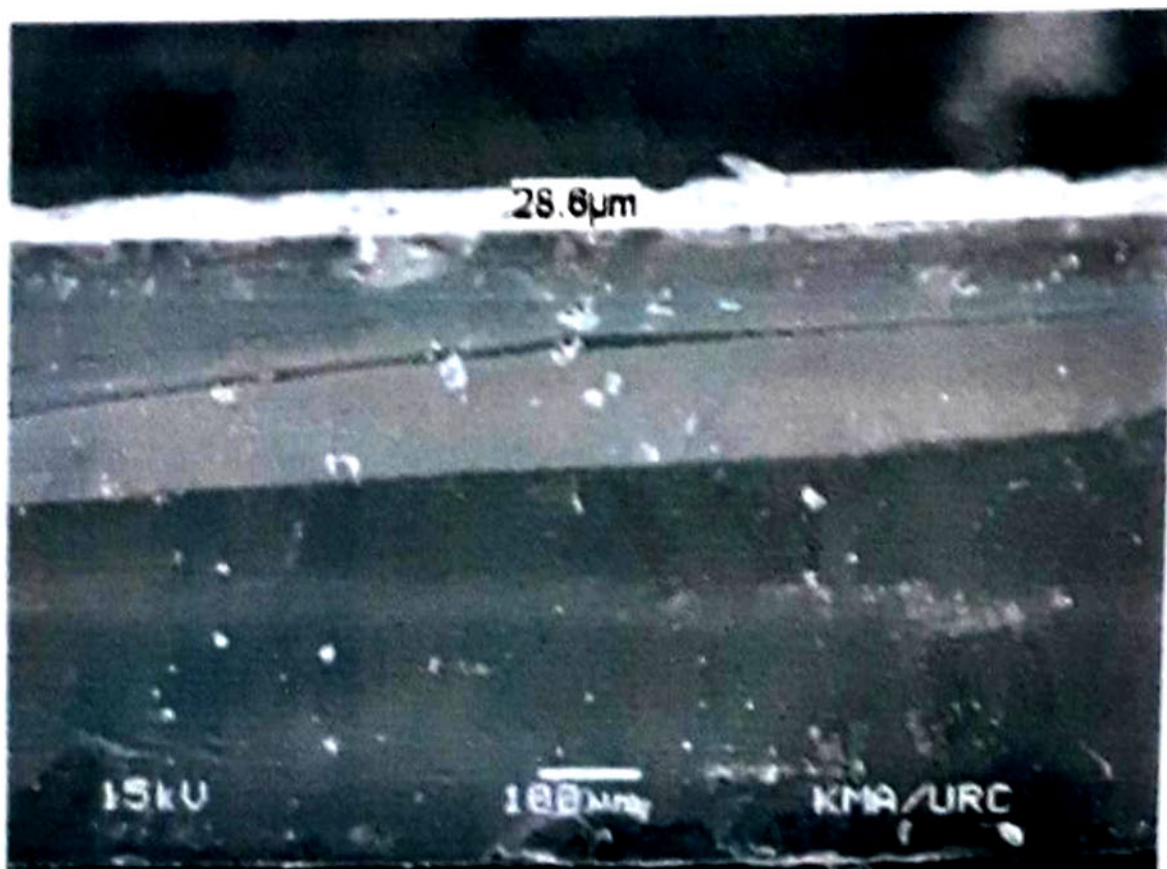


**Fig 3.4 (f) Film Thickness of SEM Image for  $\text{PbTiO}_3$  Film at  $550^\circ\text{C}$**

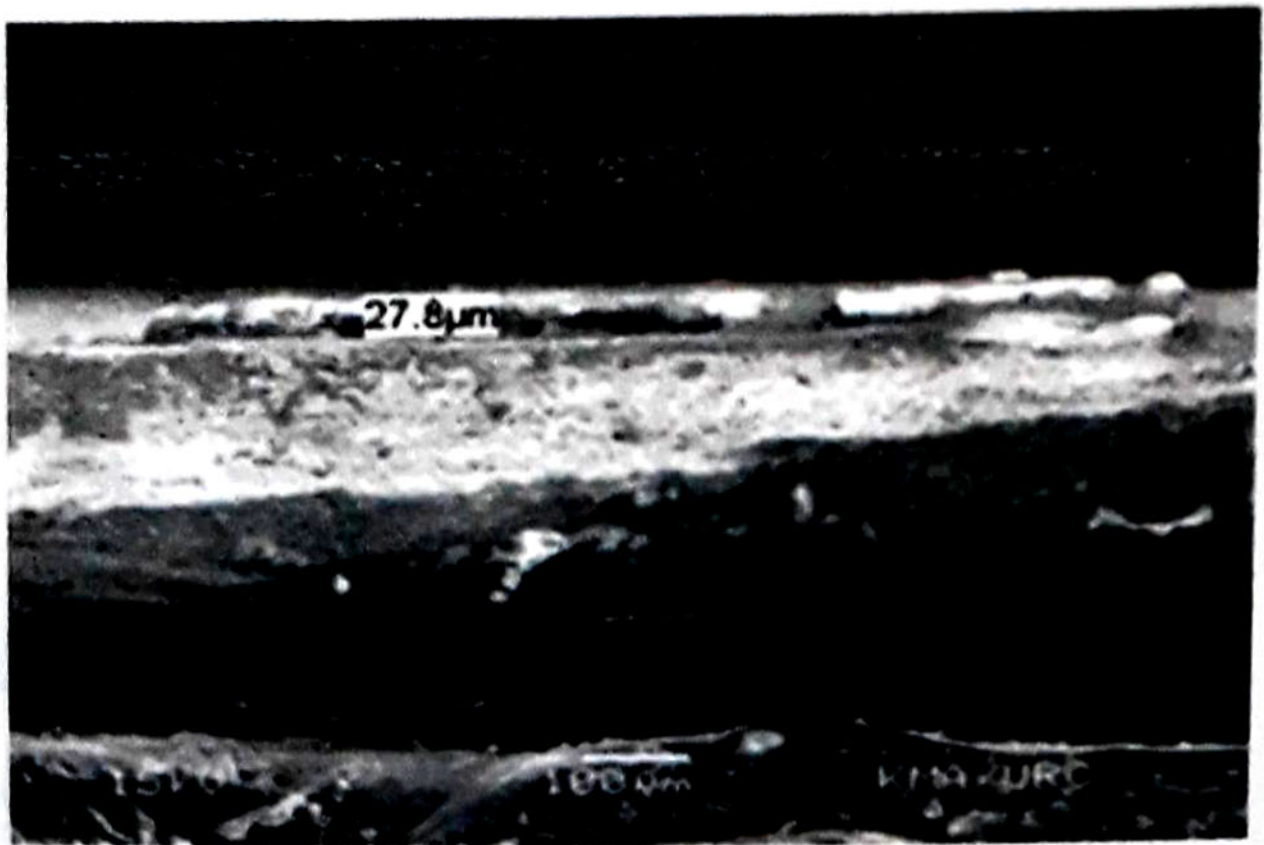


**Fig 3.4 (e) Film Thickness of SEM Image for PbTiO<sub>3</sub> Film at 500°C**

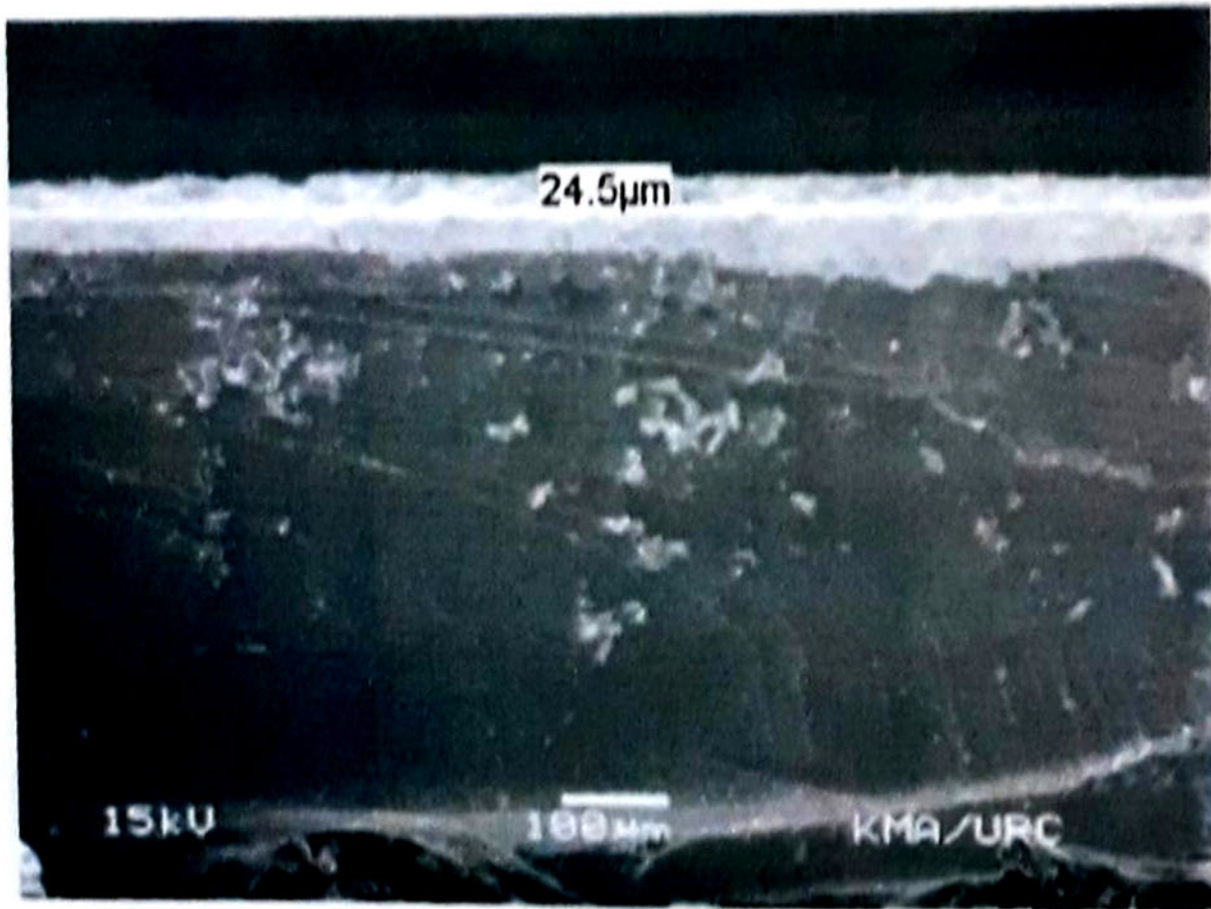


**Fig 3.4 (h) Film Thickness of SEM Image for PbTiO<sub>3</sub> Film at 650°C**

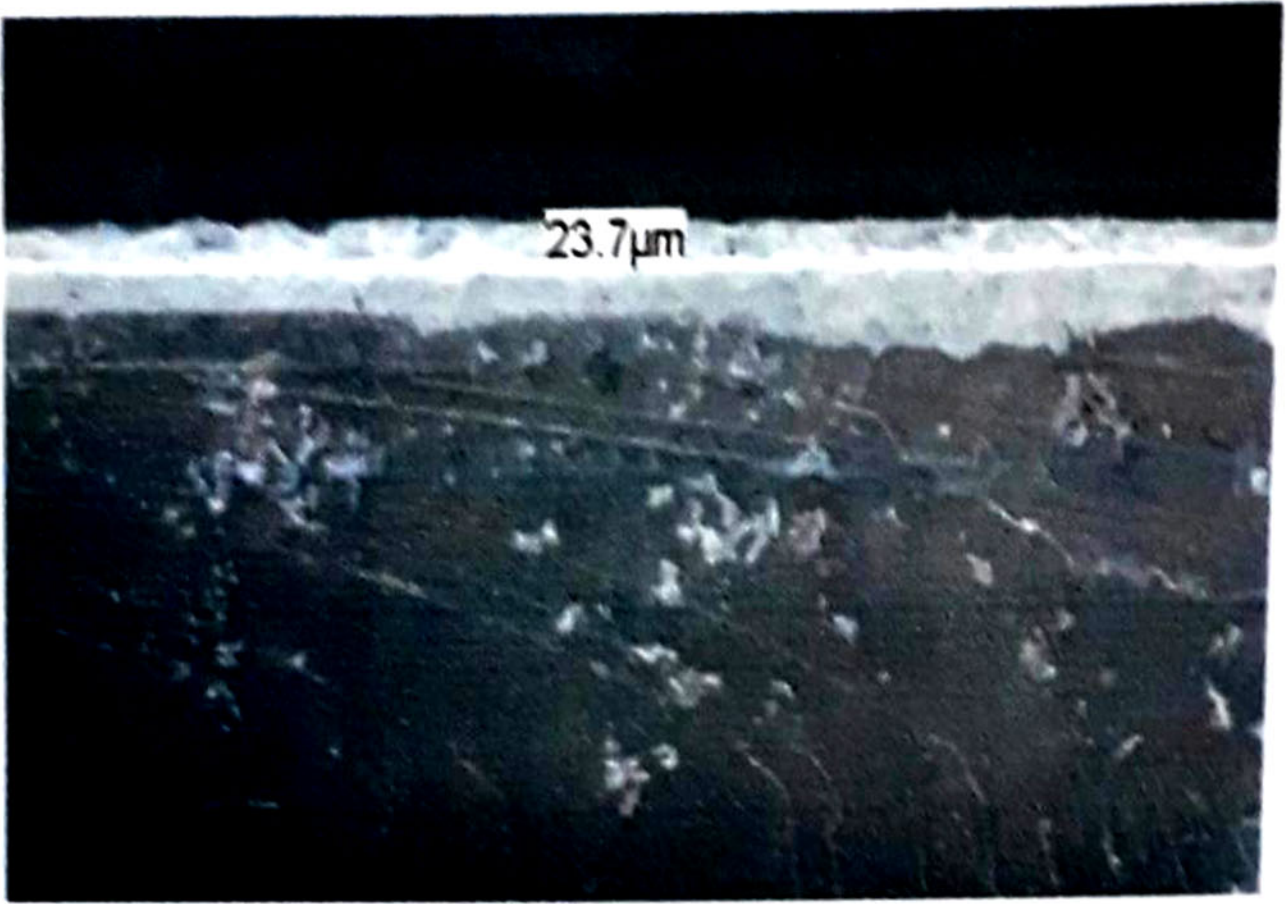


**Fig 3.4 (g) Film Thickness of SEM Image for  $\text{PbTiO}_3$  Film at  $600^\circ\text{C}$**

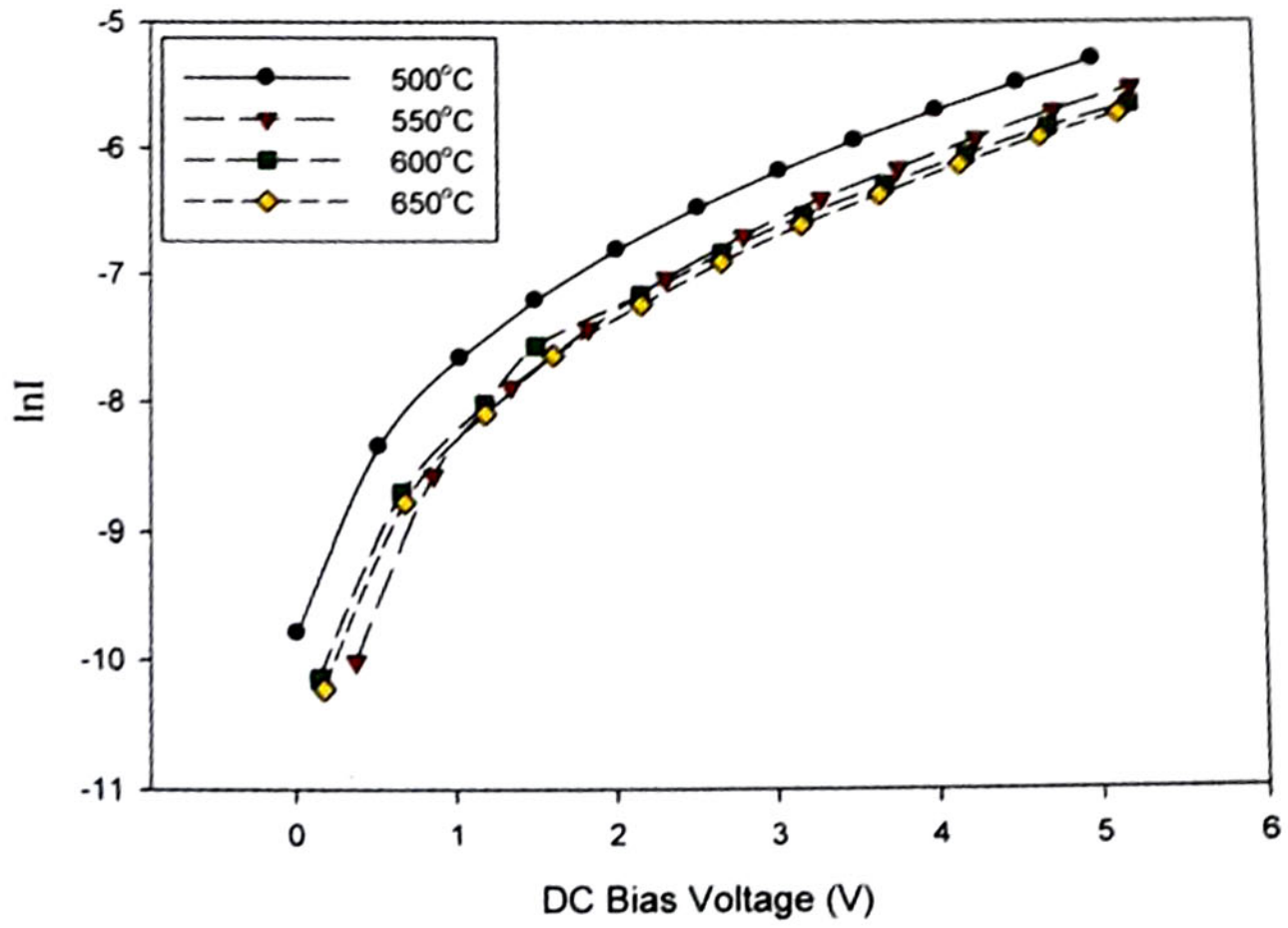


**Fig 3.5 (b)  $\ln I$ -V Characteristics of  $\text{PbTiO}_3$  Films**

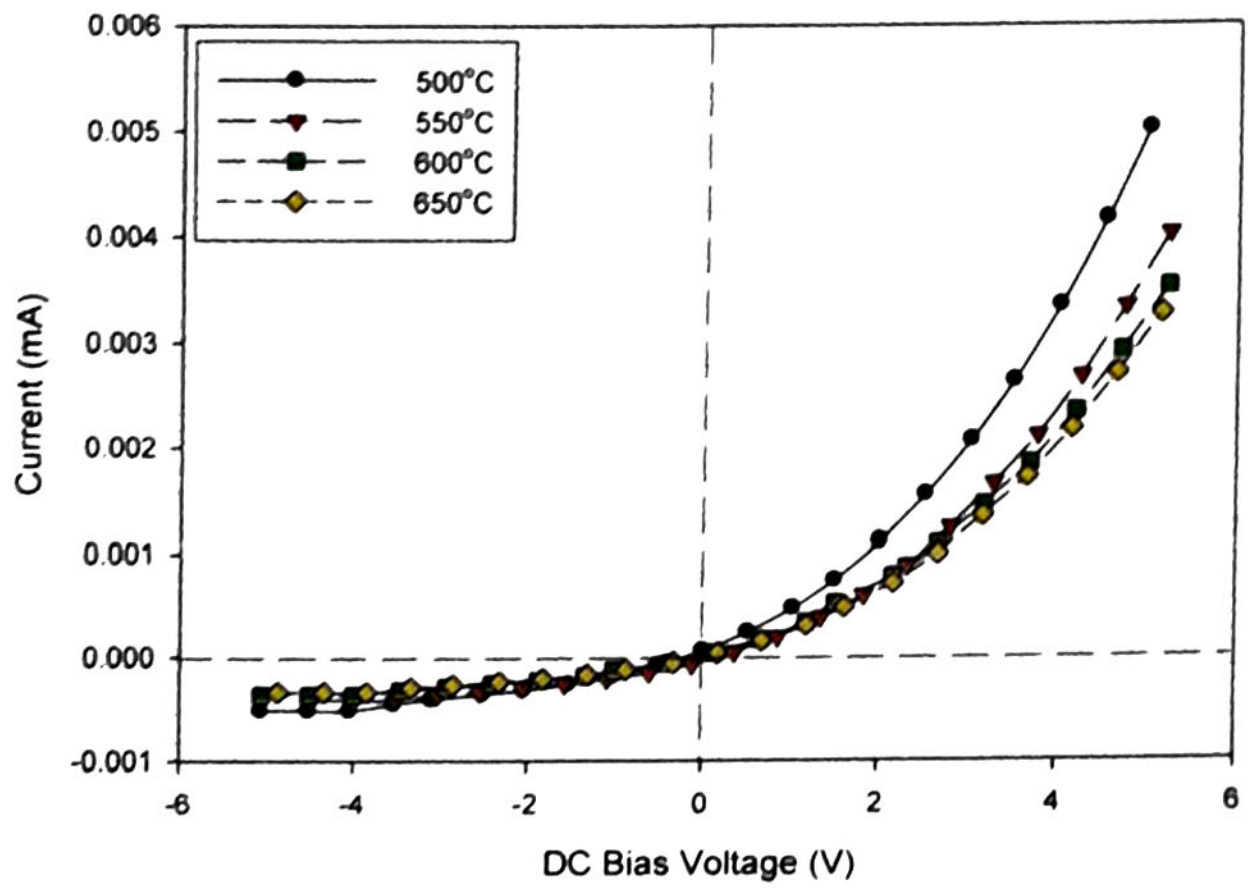


**Fig 3.5 (a) I-V Characteristics of PbTiO<sub>3</sub> Films at Different Process Temperatures**

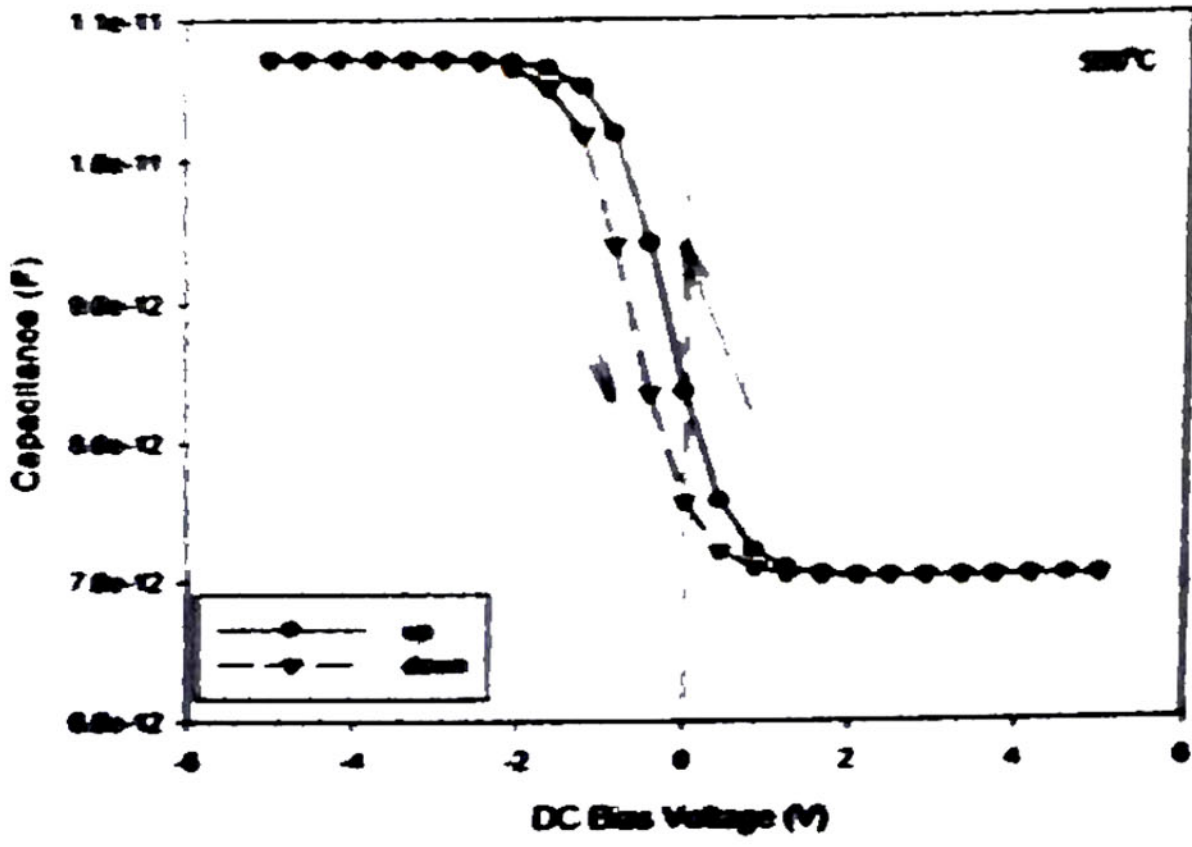


**Fig 3.6 (b) C-V Characteristics of PbTiO<sub>3</sub> Film at 550°C**

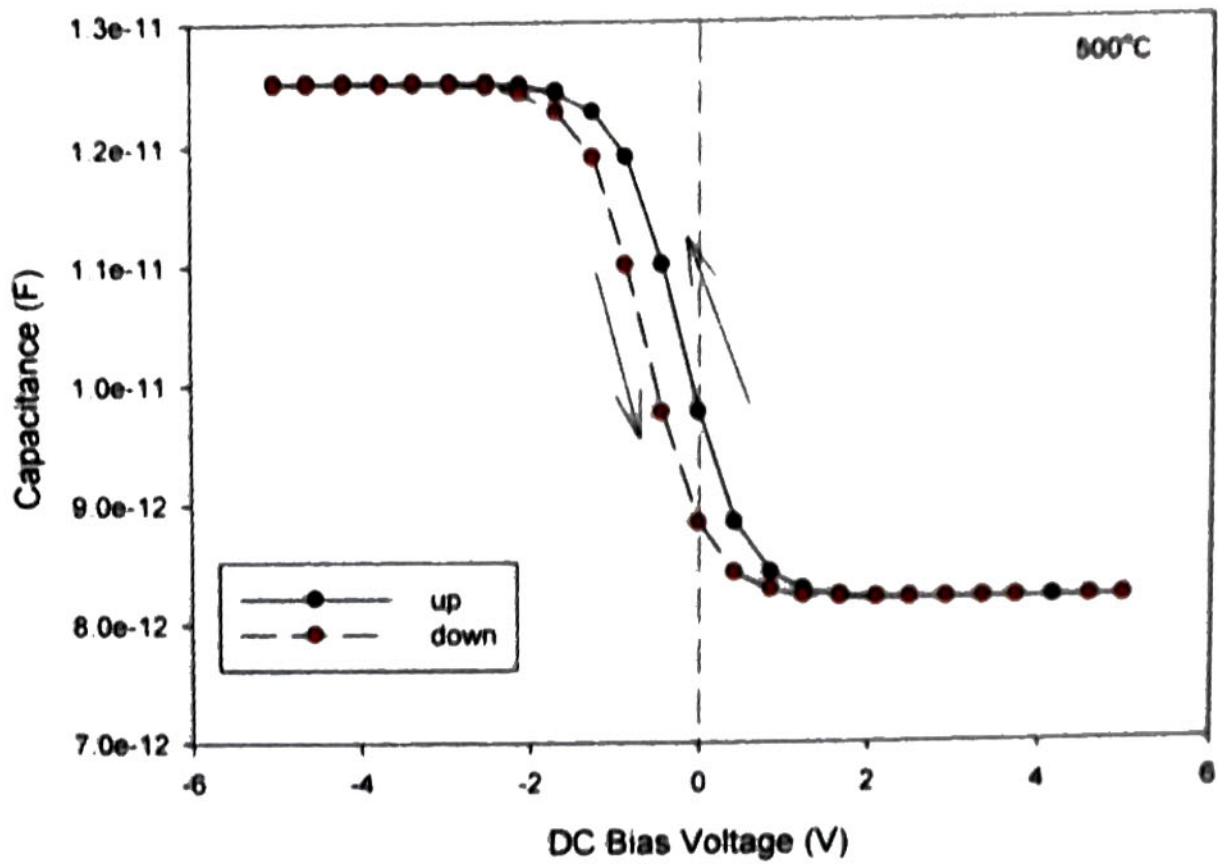


**Fig 3.6 (a) C-V Characteristics of PbTiO<sub>3</sub> Film at 500°C**

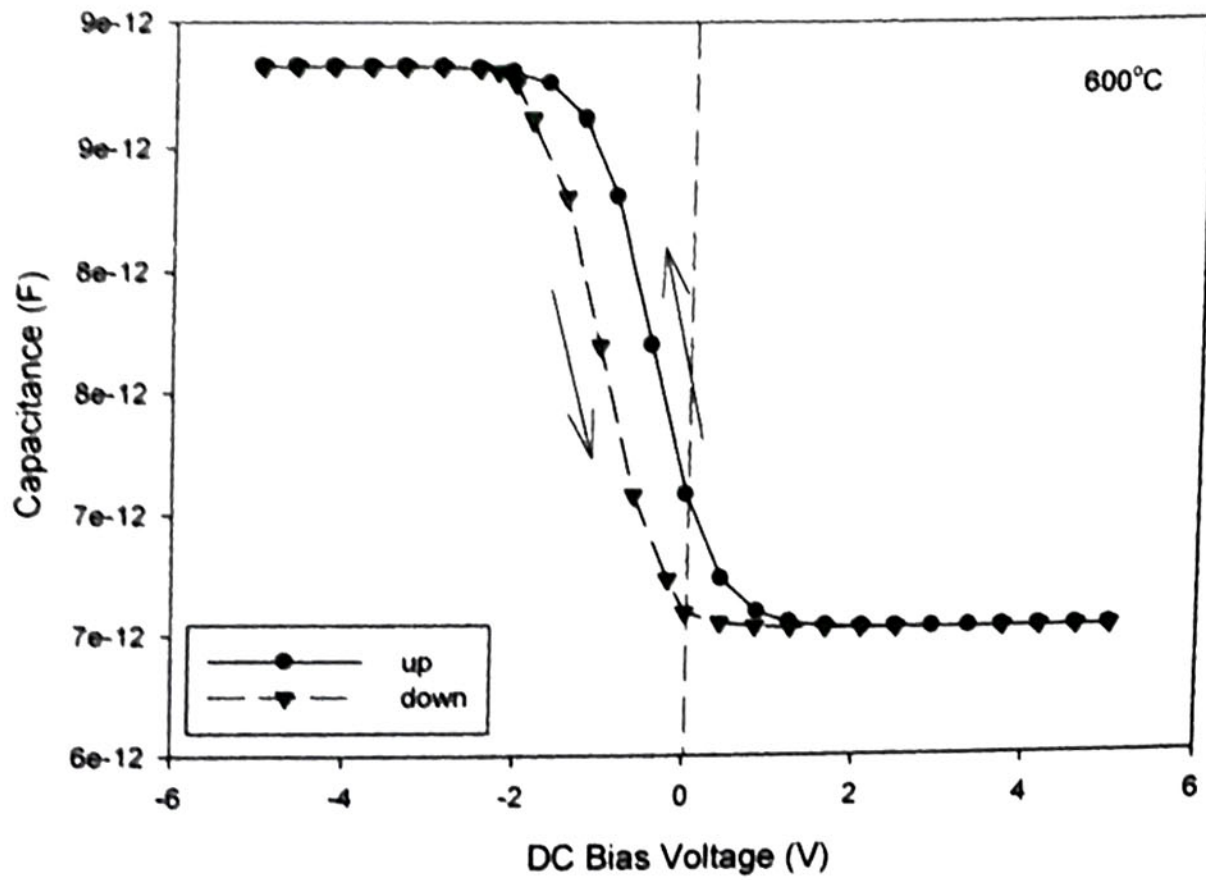


**Fig 3.6 (c) C-V Characteristics of PbTiO<sub>3</sub> Film at 600°C**

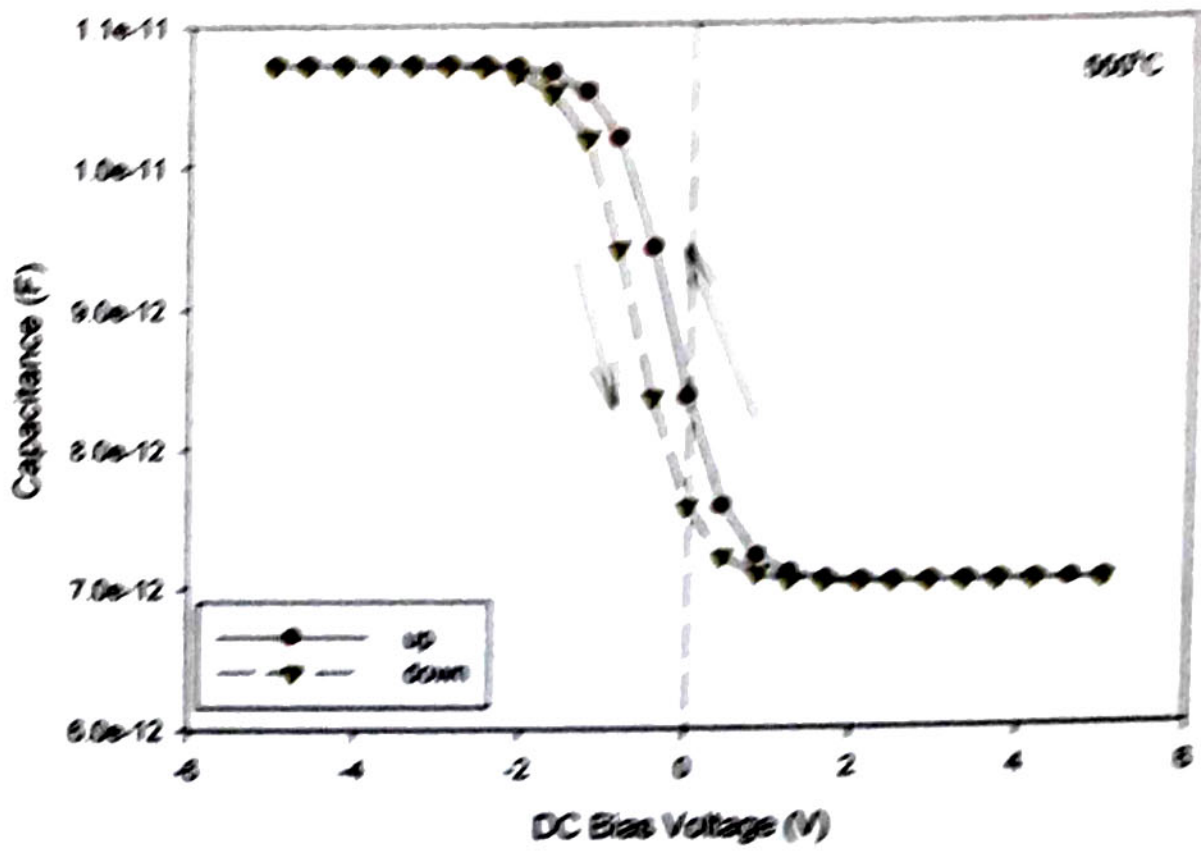


**Fig 3.6 (b) C-V Characteristics of PbTiO<sub>3</sub> Film at 550°C**

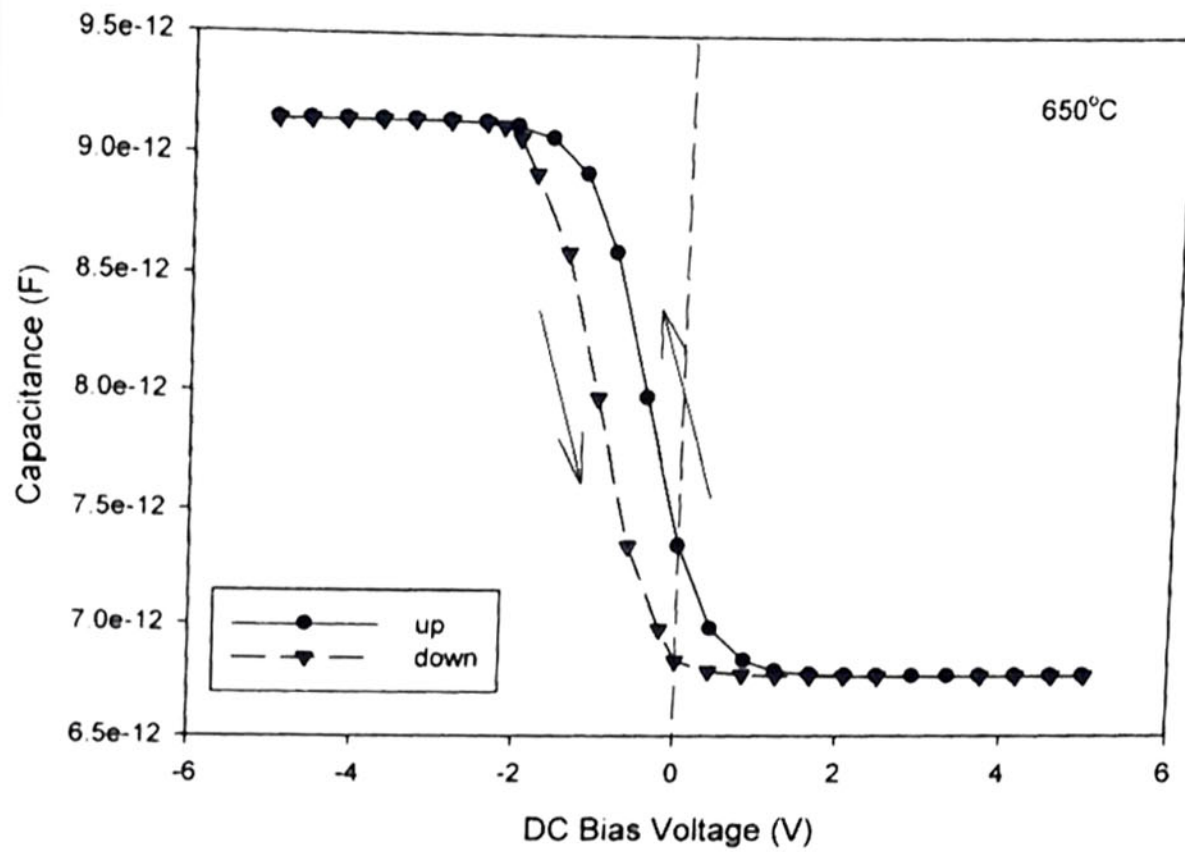


**Fig 3.6 (d) C-V Characteristics of PbTiO<sub>3</sub> Film at 650°C**

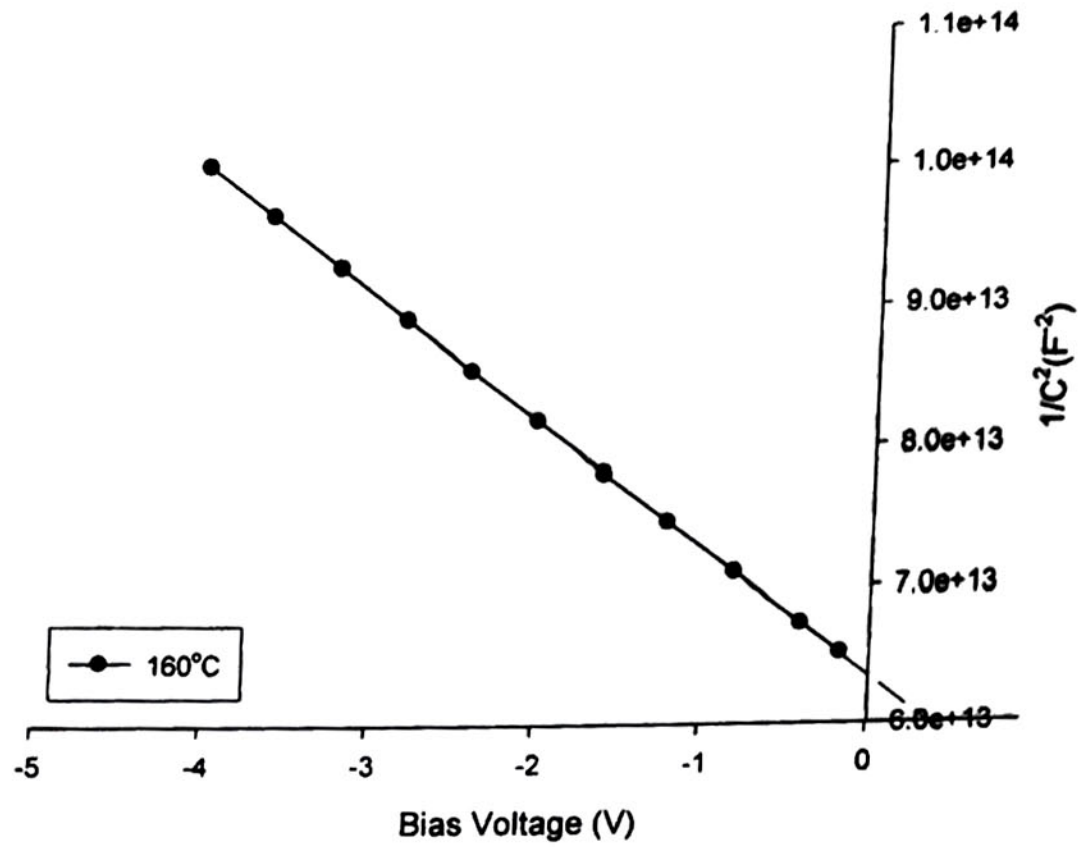


**Fig 3.7 (a)  $C^{-2}$ -V Characteristics of  $PbTiO_3$  (160°C)/ p-Si Process  
Temperature at 500°C**

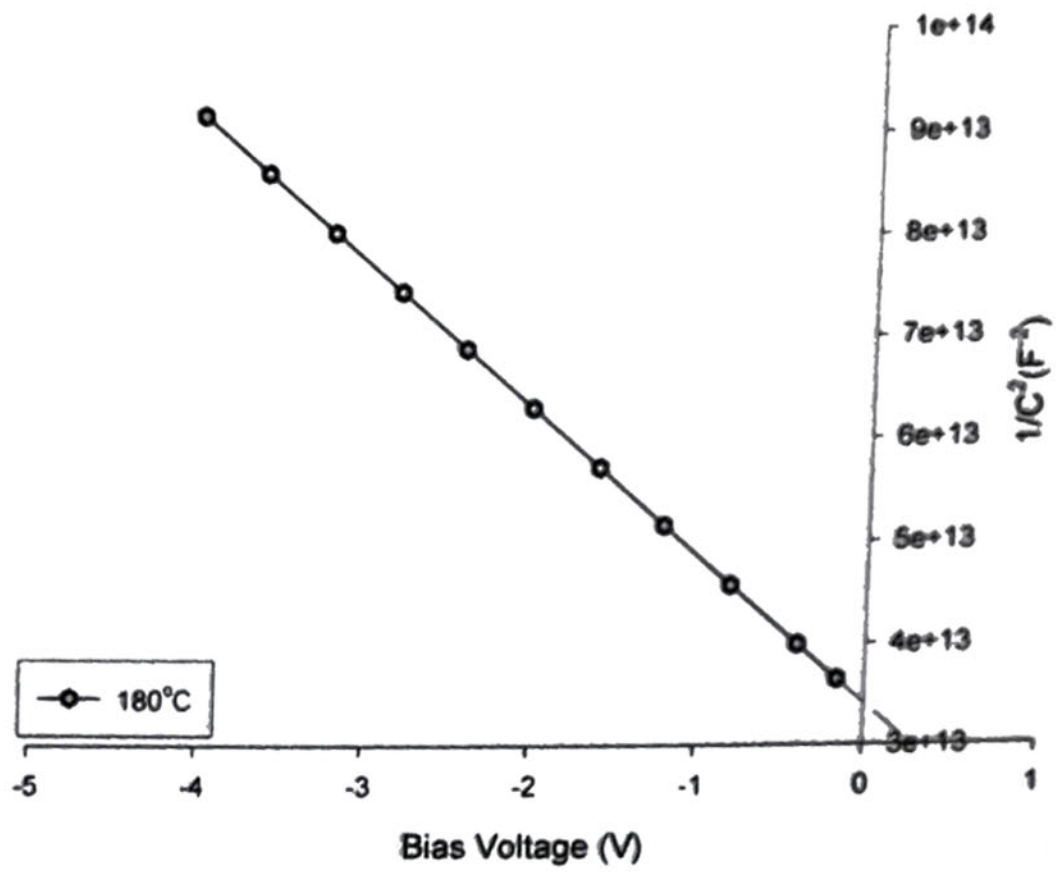


**Fig 3.7(c)  $C^{-2}$ -V Characteristics of PbTiO<sub>3</sub> (180°C)/ p-Si Process  
Temperature at 600°C**

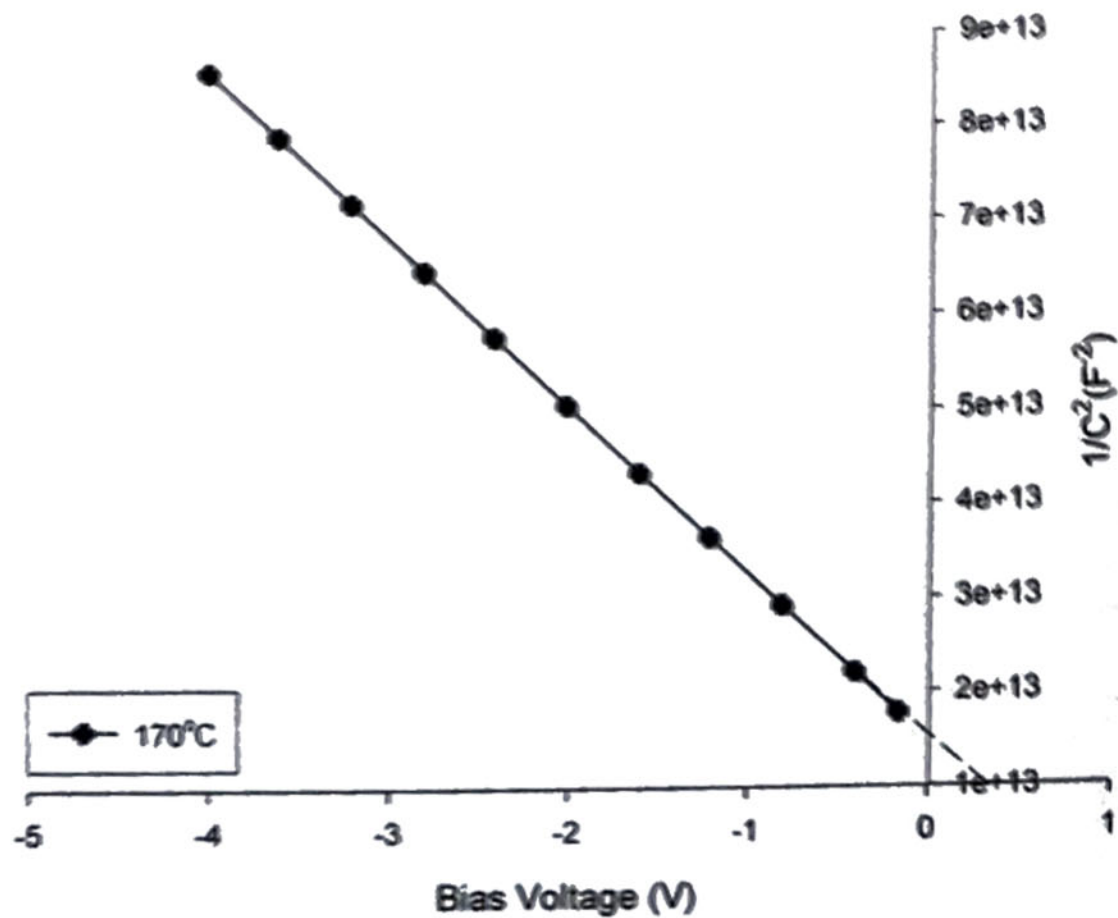


**Fig 3.7(b)  $C^{-2}$ -V Characteristics of PbTiO<sub>3</sub> (170°C)/ p-Si Process  
Temperature at 550°C**

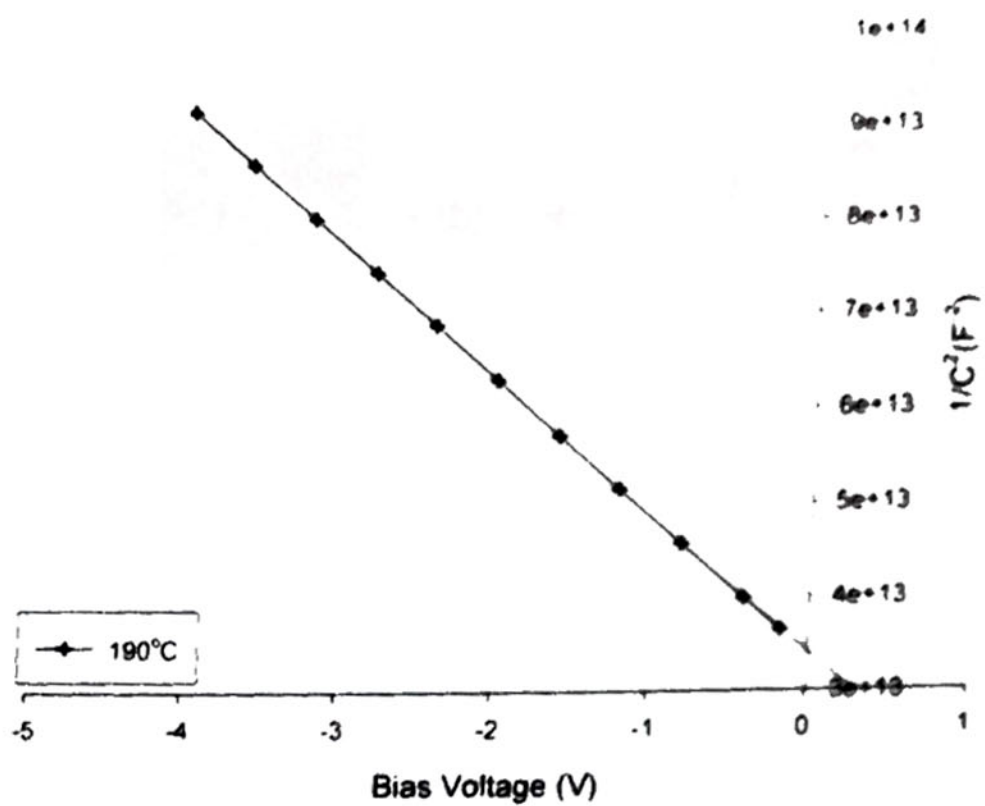


**Fig 3.7 (d)  $C^{-2}$ -V Characteristics of PbTiO<sub>3</sub> (190°C)/ p-Si Process Temperature at 650°C**

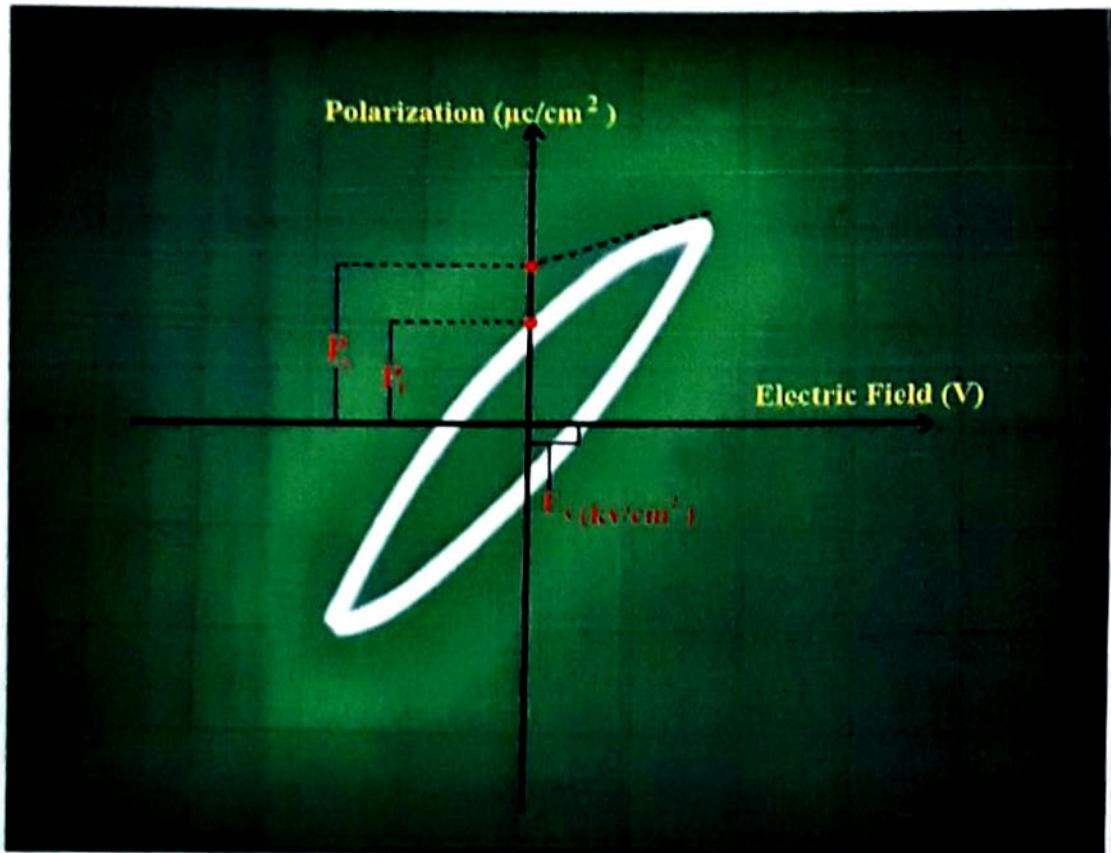


**Fig 3.8 (a) P-E Hysteresis Loop of  $\text{PbTiO}_3$  Film at  $500^\circ\text{C}$**

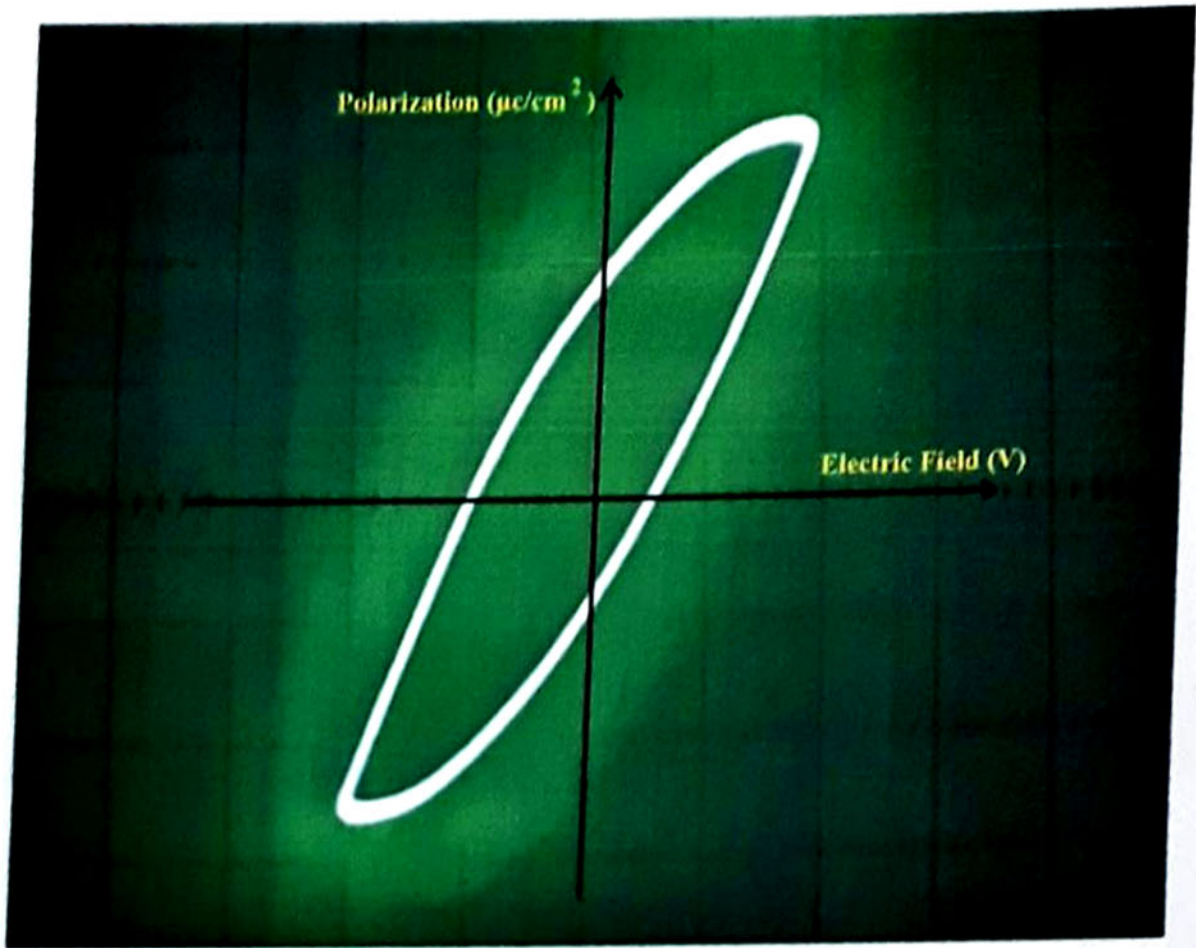


**Fig 3.8 (b) P-E Hysteresis Loop of PbTiO<sub>3</sub> Film at 550°C**

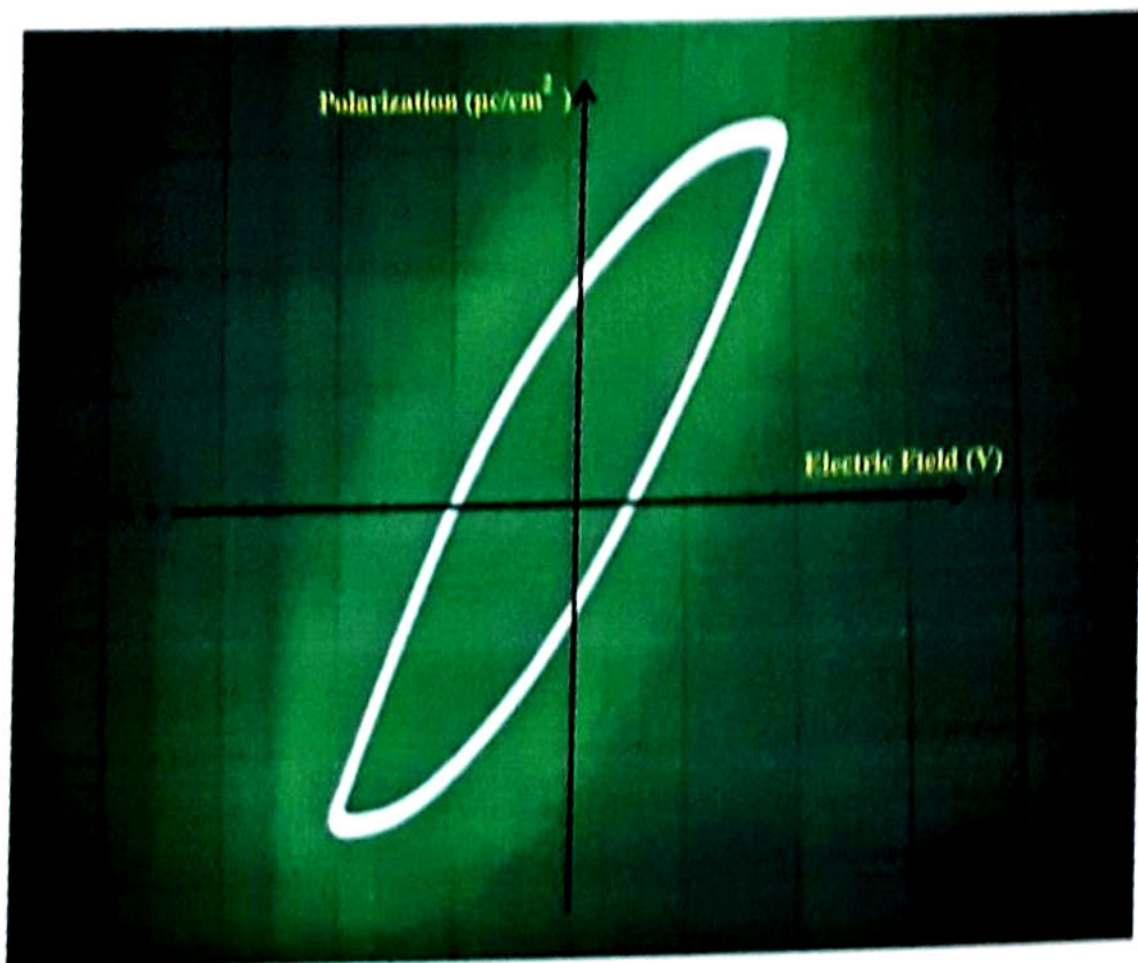


**Fig 3.8 (d) P-E Hysteresis Loop of PbTiO<sub>3</sub> Film at 650°C**

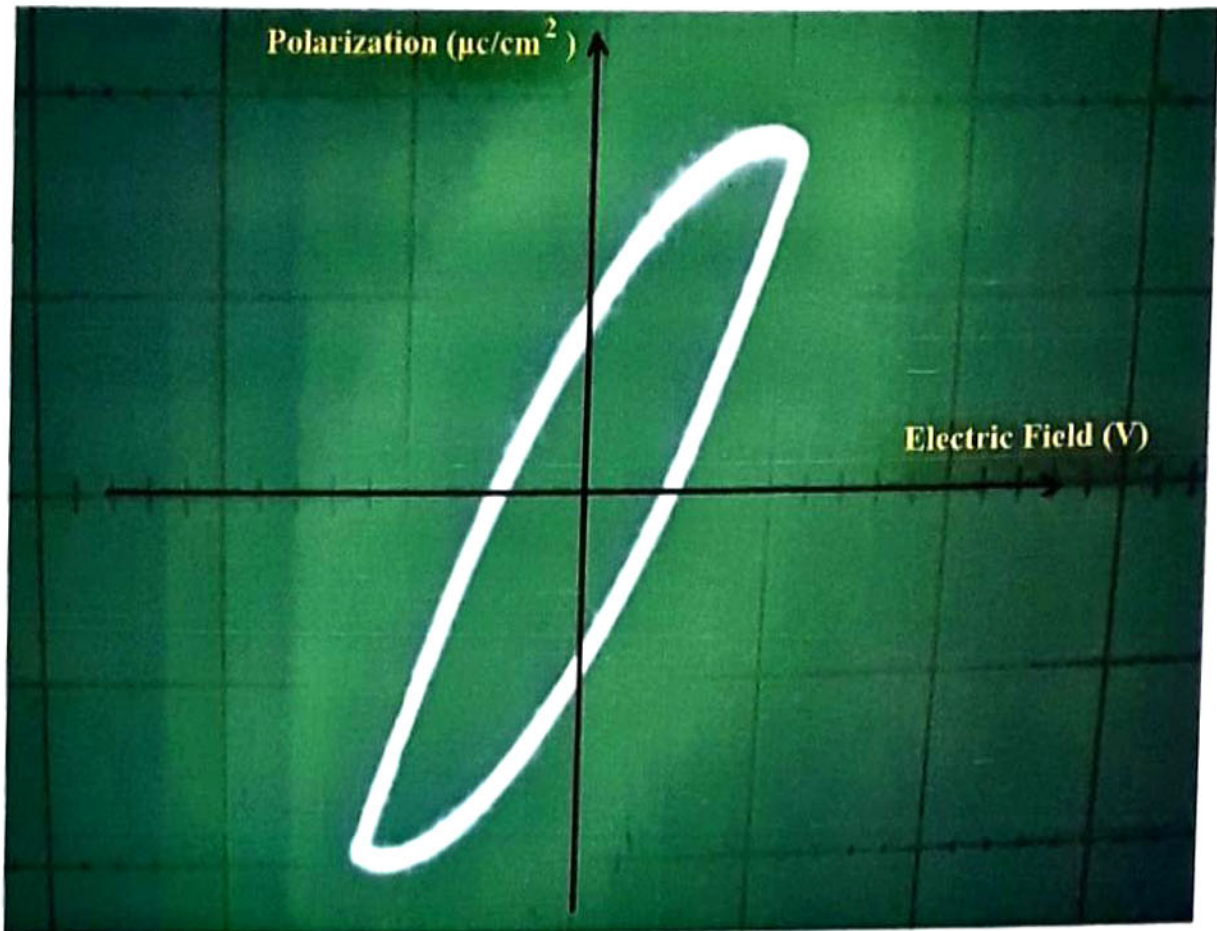


**Fig 3.8 (c) P-E Hysteresis Loop of  $\text{PbTiO}_3$  Film at  $600^\circ\text{C}$**

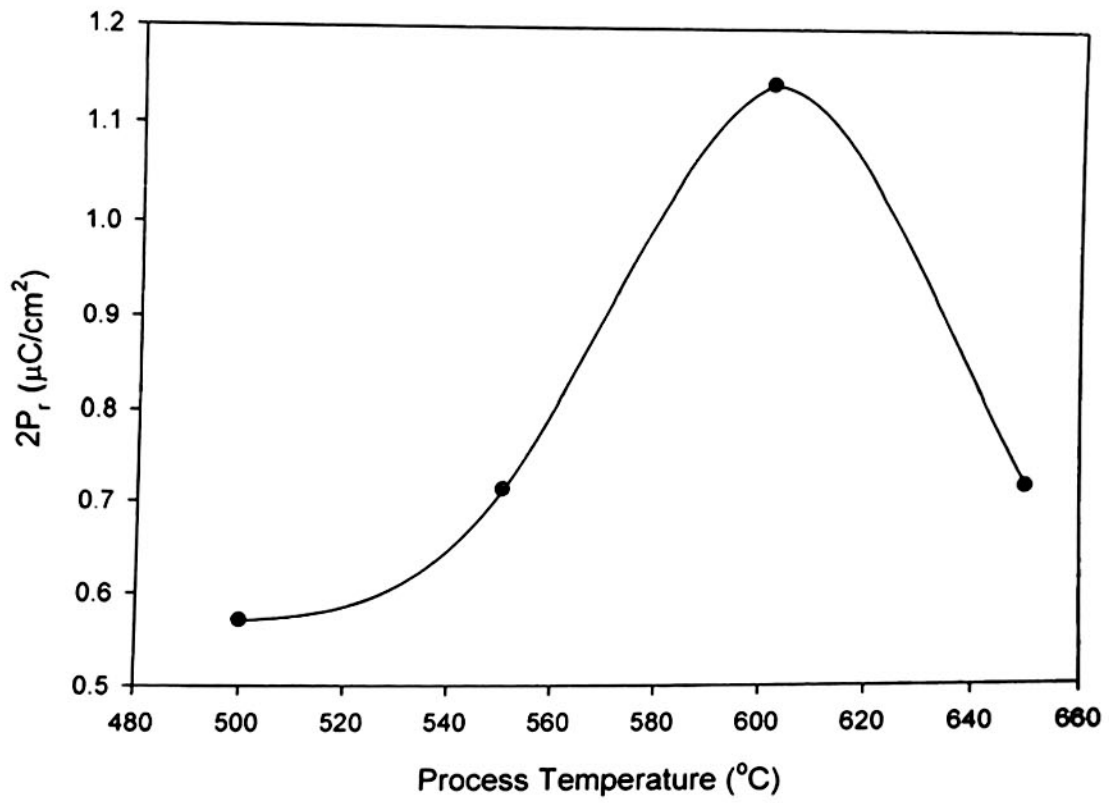


**Fig 3.9 (a) Polarization reversal at Different Process Temperatures**

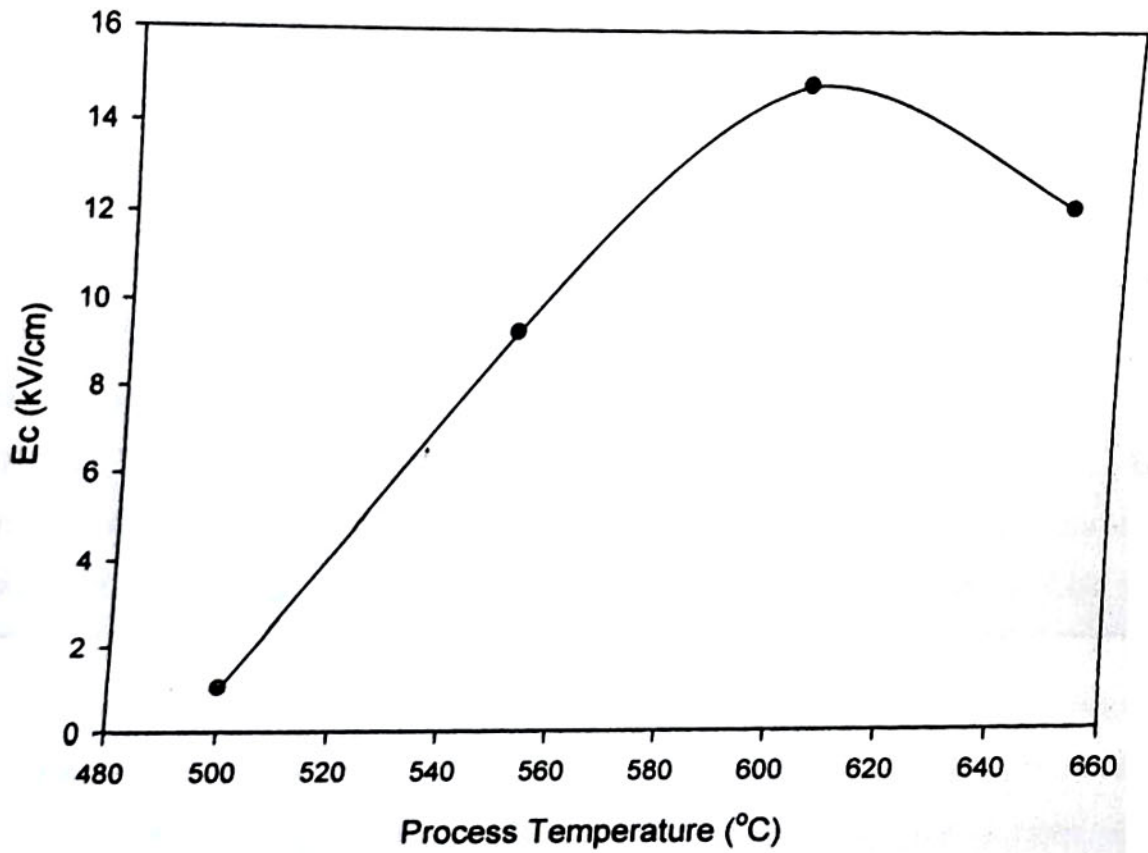


**Fig 3.9 (c) The Change in  $E_c$  with Respect to Process Temperature**

# CHAPTER IV

## CONCLUSION

Hydrothermal synthesized lead titanate powder,  $\text{PbTiO}_3$  was successfully formed at different bath temperatures with tetragonal symmetry. The smallest value of crystallite size was formed for the  $\text{PbTiO}_3$  powder at  $160^\circ\text{C}$  while the powder at  $190^\circ\text{C}$  exhibited the maximum degree of crystallite size. As a result of  $\text{PbTiO}_3$  powder analysis by SEM, the grain size was in the micrometer range. The crystallite size and grain size were much different. This fact give the polycrystallite nature of  $\text{PbTiO}_3$  specimen. C-V characteristics of  $\text{PbTiO}_3$  ceramic capacitors showed the ferroelectricity and nonvolatility of lead titanate. Also the grain morphology (film morphology) of  $\text{PbTiO}_3$  film indicated that the  $\text{PbTiO}_3$  film was obviously formed on p-Si (100) substrate at given process temperatures. According to the film thickness value, all films were said to be "thin film". From I-V characteristics of  $\text{PbTiO}_3$  films, typical p-n junction contact was formed. All zero-bias barrier heights were examined to be less than unity. All ideality factors were observed to be greater than unity, except the film at  $500^\circ\text{C}$ . There was no leakage current in the  $\text{PbTiO}_3$  film at  $500^\circ\text{C}$ . Thus, it was formed on p-Si (100) substrate with good diode nature. From C-V characteristics of  $\text{PbTiO}_3$  film at different process temperatures, hysteresis gap was clearly appeared and showed the memory function. It met the standard of the special requirements for the development of cost effective memory capacitor.  $C^2$ -V linear relationship showed the homogeneity of  $\text{PbTiO}_3$  film. All built-in-voltages were observed to be negative value and it conformed the p-type conductivity of silicon substrate. Well-defined hysteresis loop conformed the ferroelectric nature and nonvolatile memory behaviour of  $\text{PbTiO}_3$  film. The lower value of spontaneous polarization density ( $P_s$ ) and measurement polarization density ( $P_r$ ) could be explained on the basis of small dipole moment in these temperatures. This fact revealed that the  $\text{PbTiO}_3$  film exhibited the low relative dielectric constant and high loss tangent. Thus, the results obtained from this research are quite credible, appropriate, feasible and

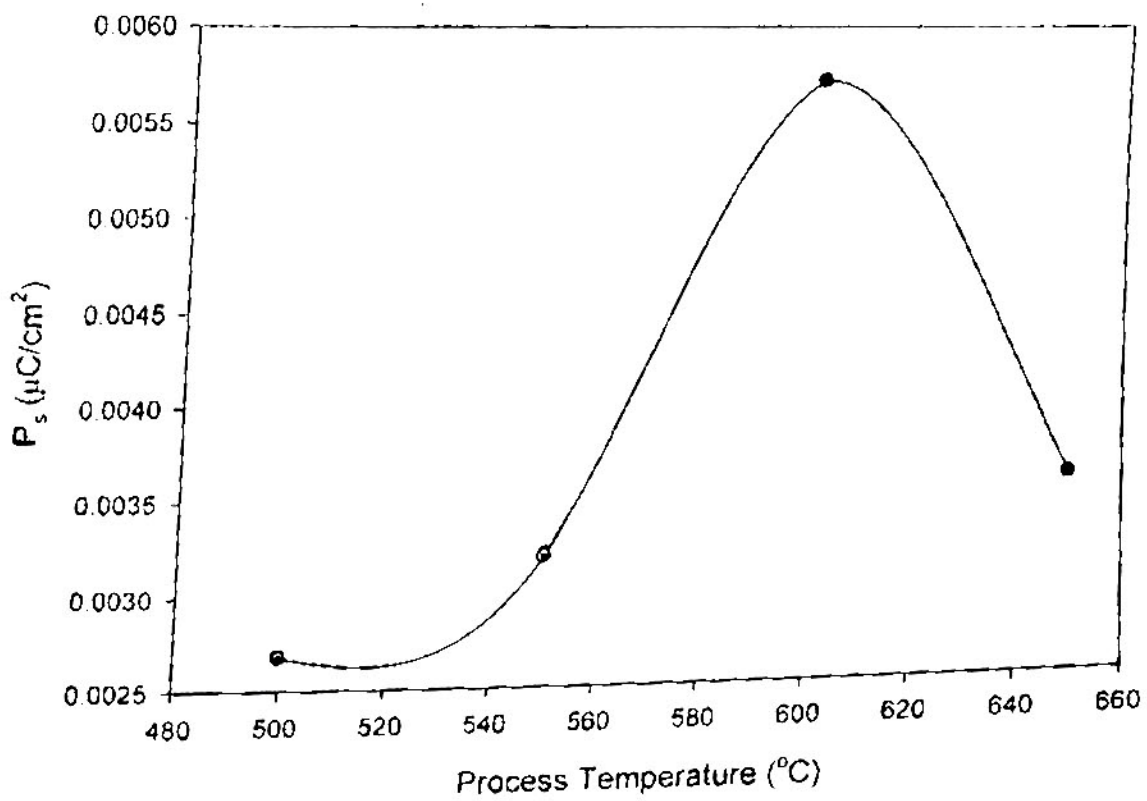


**Fig 3.9 (b) Spontaneous Polarization Density at Different Temperatures**

## REFERENCES

1. Safari A et al "Ferroelectric Ceramics: Processing, Properties & Applications" Department of Ceramic Science and Engineering (USA: Rutgers University)
2. Xu Y 1991 "Ferroelectric Materials and Their Applications"(New York: Elsevier)
3. Daghil M et al 2000 The Institution of Professional Engineers New Zealand Transactions 27 (1) 21
4. Giedeman W A 1991 IEEE Transactions on Ultrasonics, Ferroelectrics & Frequency Control 38 (6) 704
5. Lang S B 1974 "Sourcebook of Pyroelectricity" Gordon and Breach, New York
6. Sarah Beth Rickman 2003 "NNUN REU Program at Stanford Nanofabrication Facility" Chemical Engineering, Lehigh University
7. <http://en.wikipedia.org/wiki/hydrothermal-synthesis> (5-5-2010)
8. Balaraman D 2005 "Ultra - Thin Films For Low- Temperature Embedding of Decoupling capacitors into Organic Printed Wiring Boards" Dissertation, Materials Science and Engineering Department, Georgia Institute of Technology
9. <http://en.wikipedia.org/wiki/Ferroelectricity>(10-7-2010)
10. <http://en.wikipedia.org/wiki/Lead-nitrate>(10-7-2010)
11. <http://en.wikipedia.org/wiki/Titanium-dioxide>(15-9-2010)
12. <http://en.wikipedia.org/wiki/Potassium-hydroxide>(15-9-2010)
13. [http://www.mrs.org/wiki/Lead Titanate](http://www.mrs.org/wiki/Lead_Titanate)
14. <http://www.wisegeek.com/What-is-teflon.htm>(12-11-2010)
15. <http://www.wisegeek.com/What-is-stainless-steel.htm>(12-12-2010)

## External Examiner's Report

Candidate : Thin Thin Thwe

Roll No : 4 PhD Phys - 29 (2011-2012)

Thesis Title : Preparation of Hydrothermal Synthesized Lead Titanate Film  
For Non-Volatile Memory Device Application

The doctoral research conducted by the PhD (Physics) candidate, Thin Thin Thwe, is in the area of Materials Science - a leading edge branch of the physics discipline. In the present work she had synthesized a Lead Titanate film and measured its electrical properties. Surface morphology of the sample had also been studied through Scanning Electron (SE) Microscopy. The results of her experiments are quite good.

Tin Aung

Dr Tin Aung

Professor

Retired HOD

Department of Physics

University of Yangon

Based upon her performance in the viva voce examination and the quality of her PhD dissertation, the External Examiner assesses that the candidate is worthy of the PhD degree for which she is, unreservedly, recommended.

## Referee's Report

**Candidate : THIN THIN THWE**  
**Roll No. : 4 PhD Phys-29 (2011-2012)**  
**Thesis Title : Preparation of Hydrothermal Synthesized Lead Titanate Film for Non-Volatile Memory Device Application**

The dissertation submitted by the candidate, Thin Thin Thwe, is well-documented report of the results from her research work which interests the materials scientists. Her research involved in Preparation of Hydrothermal Synthesized Lead Titanate Film for Non-Volatile Memory Device Application.

The useful and credible findings resulted from the research can be applied in making more compact products. The choice of techniques the candidate had made is appropriate, accurate and the experiment was well-organized. This finding will play vitally important role in Materials Science.

It is fully recommended that the candidate is worth being conferred the degree of the Doctor of Philosophy in Physics.

April 10, 2012



**Dr Hla Pe**  
**Rector (Rtd.)**  
**Mawlamyaing University**

applicable in use for single capacitor in nonvolatile ferroelectric random access memory (NVFRAM).